

https://dspace.org/

Comparative anatomy of the caudate nucleus in canids and felids Associations with brain size curvature crosssectional properties and behavioral ecology

Michael Foster; Sai Dwibhashyam; Devan Patel; Kanika Gupta; Brendon Billings ...

WILEY-BLACKWELL
https://hdl.handle.net/10539/42579
WOS

Downloaded from a DSpace repository. https://dspace.org/

Check for updates

Received: 21 August 2023 | Revised: 30 March 2024 | Accepted: 16 April 2024

DOI: 10.1002/cne.25618

RESEARCH ARTICLE

JCN RESEARCH IN SYSTEMS NEUROSCIENCE THE JOURNAL OF COMPARATIVE NEUROLOGY WILEY

Comparative anatomy of the caudate nucleus in canids and felids: Associations with brain size, curvature, cross-sectional properties, and behavioral ecology

Michael Foster[1] | Sai Dwibhashyam[1] | Devan Patel[1] | Kanika Gupta[1] | Olivia C. Matz[1] | Brendon K. Billings[2] | Kathleen Bitterman[1] | Mads Bertelson[3] | Cheuk Y. Tang[4] | Rogier B. Mars[5,6] | Mary Ann Raghanti[7] | Patrick R. Hof[8,9] | Chet C. Sherwood[10] | Paul R. Manger[2] | Muhammad A. Spocter[1,2,11]

[1]Department of Anatomy, Des Moines University, West Des Moines, Iowa, USA

[2]School of Anatomical Sciences, Faculty of Health Sciences, University of the Witwatersrand, Johannesburg, Republic of South Africa

[3]Center for Zoo and Wild Animal Health, Copenhagen Zoo, Frederiksberg, Denmark

[4]Departments of Radiology and Psychiatry, BioMedical Engineering and Imaging Institute, Icahn School of Medicine at Mount Sinai, New York, New York, USA

[5]Wellcome Centre for Integrative Neuroimaging, FMRIB, Nuffield Department of Clinical Neurosciences, University of Oxford, Oxford, UK

[6]Donders Institute for Brain, Cognition and Behavior, Radboud University Nijmegen, Nijmegen, The Netherlands

[7]Department of Anthropology and School of Biomedical Sciences, Kent State University, Kent, Ohio, USA

[8]Nash Family Department of Neuroscience and Friedman Brain Institute, Icahn School of Medicine at Mount Sinai, New York, New York, USA

[9]New York Consortium in Evolutionary Primatology, New York, New York, USA

[10]Department of Anthropology and Center for the Advanced Study of Human Paleobiology, The George Washington University, Washington, District of Columbia, USA

[11]College of Veterinary Medicine, Department of Biomedical Sciences, Iowa State University, Ames, Iowa, USA

Correspondence
Muhammad A. Spocter, Department of Anatomy, Des Moines University, 8025 Grand Avenue, West Des Moines, IA 50266, USA.
Email: Muhammad.spocter@dmu.edu

Associate editor: Kathleen Rockland.

Funding information
Biotechnology and Biological Sciences Research Council, Grant/Award Number: BB/N019814/1; Carnegie Corporation of New York; Iowa STEM BEST; South African National Research Foundation

Abstract

The evolutionary history of canids and felids is marked by a deep time separation that has uniquely shaped their behavior and phenotype toward refined predatory abilities. The caudate nucleus is a subcortical brain structure associated with both motor control and cognitive, emotional, and executive functions. We used a combination of three-dimensional imaging, allometric scaling, and structural analyses to compare the size and shape characteristics of the caudate nucleus. The sample consisted of MRI scan data obtained from six canid species (*Canis lupus lupus*, *Canis latrans*, *Chrysocyon brachyurus*, *Lycaon pictus*, *Vulpes vulpes*, *Vulpes zerda*), two canid subspecies (*Canis lupus familiaris*, *Canis lupus dingo*), as well as three felids (*Panthera tigris*, *Panthera uncia*, *Felis silvestris catus*). Results revealed marked conservation in the scaling and shape attributes of the caudate nucleus across species, with only slight deviations. We hypothesize that observed differences in caudate nucleus size and structure for the domestic canids are reflective of enhanced cognitive and emotional pathways that possibly emerged during domestication.

© 2024 Wiley Periodicals LLC.

KEYWORDS
Carnivora, caudate nucleus, RRID:SCR_002010, RRID:SCR_003430, RRID:SCR_005988, scaling, brain

1 | INTRODUCTION

Since their evolutionary divergence in the early to late Eocene, canids and felids have developed separate morphological and behavioral adaptations, particularly focused on honing predatory abilities (van Valkenberg, 1985). This refined predatory prowess (Nowak, 2005) has skewed our perception of the comparative social and cognitive behaviors of the Carnivora. This bias has not only limited the scope of our knowledge (Tensen, 2018) but also has potentially permitted (through a lack of action) the ongoing population decline for many of these mammals.

The recent resurgence of interest in the domestication process has reignited studies on the comparative morphology (Lyras, 2009), genetics, and behavioral ecology of wild species to contextualize the domestication process (Spocter et al., 2018), especially so in wild canids and felids (e.g., Chengetenai et al., 2020; Grewal et al., 2020; Jacobs et al., 2018; Nelson et al., 2024; Nguyen et al., 2020; Oddes et al., 2023; Sacco et al., 2023). Comparisons using this phylogenetic context (See Figure 1) allows for the study of trait evolution between species and helps us reconstruct the evolutionary history of the trait understudy. In addition, comparative behavioral and neuroimaging studies in domestic carnivores have posed serious questions about the apparent uniqueness of certain behavioral traits in domesticates and their neuroanatomical basis compared to wild-type relatives (e.g., Hecht et al., 2019, 2021). One prime example of this has been the emerging observation from functional imaging studies in domestic canids (*Canis lupus familiaris*). Through the use of awake state functional magnetic resonance imaging (fMRI), several recent studies have revealed surprising similarities in the neural pathway of reward prediction and the processing of positive valence stimuli in humans and domestic canids (Andics & Miklósi, 2018; Andics et al., 2016; Berns et al., 2015; Berns et al., 2017; Cook et al., 2014, 2016; Cuaya et al., 2016; Huber & Lamm, 2017; Jia et al., 2014; Karl et al., 2020)

The caudate nucleus is known to be involved in the inhibition and facilitation of voluntary movement (Matz & Spocter, 2022) as well as playing an important role in cognitive processes, particularly decision-making based on affective or reward processes and the control of executive functions (Balleine et al., 2007; Haber, 2003; Haber et al., 1995; Lauwereyns et al., 2002; Tanaka et al., 2006, 2008). The caudate nucleus, through its various connections with limbic and prefrontal cortical regions (e.g., Alexander & Crutcher, 1990, Nambu, 2008), is involved in many non-motor functions, including memory, motivation, reward, emotion, and associative learning (e.g., Balleine et al., 2007; Doi et al., 2020; Fischer et al., 2006; Lauwereyns et al., 2002; Seger & Cincotta, 2005; Tanaka et al., 2008). The caudate nucleus can be structurally and functionally differentiated into three major parts: an anterior head, a body, and a tail (see Figure 2; Kotz et al., 2013). Although projections from the cerebral cortex to the caudate nucleus (and associated putamen) undergo a wide degree of divergence (Wise et al., 1996), these connections are differentiated into separate corticostriatal loops, with the anterior head of the caudate forming part of the "cognitive" loop, while the tail of the caudate forms part of the "visual" loop (Lawrence et al., 1998; Middleton & Stick, 1996).

To date, no studies have examined the comparative volumetrics of the caudate nucleus in carnivores. Thus, there is a gap in our knowledge regarding how caudate nucleus dimensions and shape differences across canids and felids are related to variation in brain size or behavioral ecology. Here we provide volumetric data on the shape and size parameters of the caudate nucleus in canids and felids.

2 | MATERIALS AND METHODS

2.1 | Specimens

This data set consists of 12 subjects obtained from captive populations and representing nine Carnivora species, including six wild canid species (*Canis lupus lupus* $N = 1$ adult male; *Canis latrans* $N = 1$ adult female; *Chrysocyon brachyurus* $N = 1$ adult male; *Lycaon pictus* $N = 1$, adult male; *Vulpes vulpes* $N = 1$, adult male; *Vulpes zerda* $N = 1$, adult male), two wild felid species (*Panthera uncia*, $N = 1$, male 6-year old; *Panthera tigris* $N = 1$, female 12-year old), two domestic canids (*C. lupus familiaris*, $N = 2$, male 9-month old; female 2-year old), one feral canid (*Canis lupus dingo* $N = 1$, male adult), and one domestic felid (*Felis silvestris catus* $N = 1$, adult female). A complete species list is included in Table 1, and their phylogenetic relationships are shown in Figure 1. In the following, we provide an overview of the image acquisition process.

2.2 | MRI acquisition

Magnetic resonance imaging was performed on the whole brains of 12 carnivore species. Whole brain and caudate volume data were obtained through segmentation procedures. All scanning was carried out in strict accordance with the recommendations in the Guide for the Care and Use of Laboratory Animals of the National Institutes of Health and approved by the Institutional Animal Care and Use Committees of Des Moines University, as well as the Animal Ethics and Screening Committee (AESC) of the University of the Witwatersrand (AESC No. 2012/53/01). MR images were obtained through ongoing

10969861, 2024, 5, Downloaded from https://onlinelibrary.wiley.com/doi/10.1002/cne.25618 by South African Medical Research, Wiley Online Library on [31/07/2024]. See the Terms and Conditions (https://onlinelibrary.wiley.com/terms-and-conditions) on Wiley Online Library for rules of use; OA articles are governed by the applicable Creative Commons License

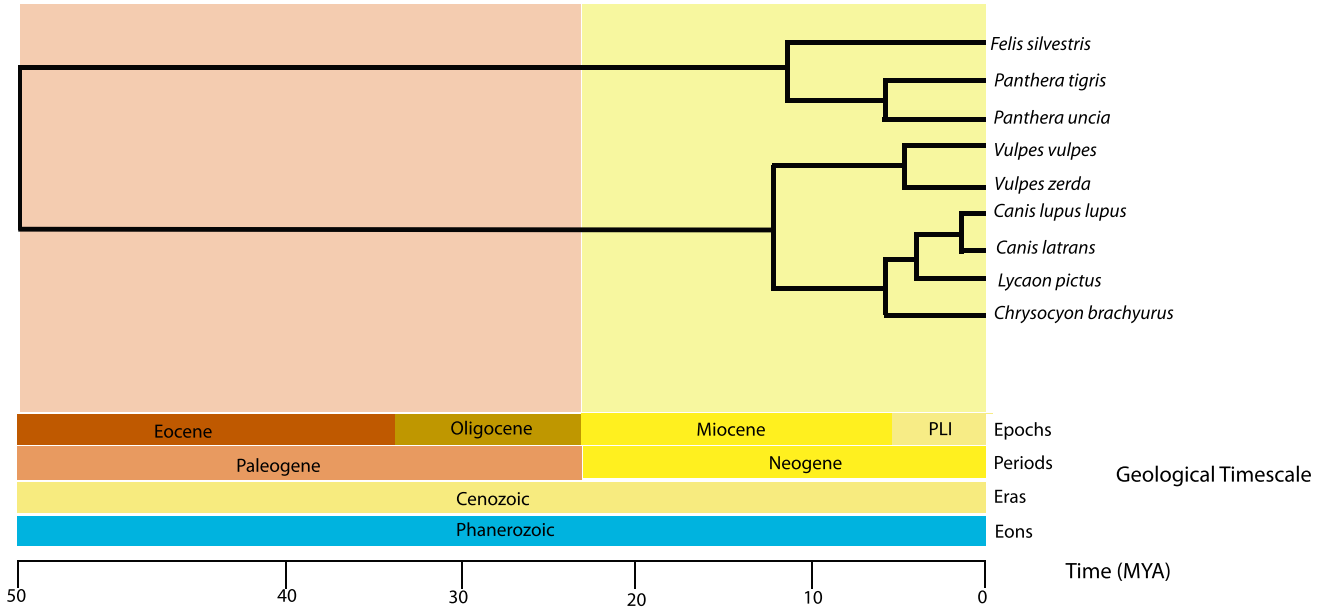

FIGURE 1 Phylogeny used in the implementation of phylogenetic generalized least squares (PGLS). PGLS was performed used the caper package (Orme et al., 2013). The phylogeny was constructed using data based on the mammalian super-tree (Nyakatura & Bininda-Emonds, 2012) as well as reference to the open-source resource TimeTree.org.

TABLE 1 Species list and associated brain and caudate mass data measured in grams (g).

Taxonomic family	Species	Common name/ specimen number	Brain mass (g)	Total caudate mass (g)	Mass of the caudate head (g)	Mass of the caudate body (g)
Felidae	*Felis silvestris catus*	Domestic cat	25.39	0.43	0.04	0.16
Felidae	*Panthera tigris*	Siberian tiger/PT1	231.24	2.57	0.38	0.62
Felidae	*Panthera uncia*	Snow leopard	69.09	1.02	0.10	0.39
Canidae	*Vulpes vulpes*	Red fox/VV1	45.15	0.83	0.07	0.26
Canidae	*Vulpes zerda*	Fennec fox/VZ1	16.27	0.34	0.04	0.13
Canidae	*Canis lupus lupus*	European wolf/CLL1	139.76	2.08	0.17	0.75
Canidae	*Chrysocyon brachyurus*	Maned wolf/CB2	91.29	1.35	0.11	0.50
Canidae	*Canis lupus familiaris*	Beagle/CF2	75.09	1.38	0.17	0.50
Canidae	*Canis lupus familiaris*	Beagle/CF1	61.30	1.08	0.15	0.34
Canidae	*Lycaon pictus*	African wild dog/LP1	132.82	1.75	0.20	0.66
Canidae	*Canis latrans*	Coyote/CL1	75.34	1.21	0.20	0.35
Canidae	*Canis lupus dingo*	Dingo/D1	83.78	1.23	0.18	0.42

Note: Volumes were converted to mass through use of the specific gravity of brain tissue (1.036 g/cm^3; Stephan, 1960).

collaborations with two imaging facilities: the Department of Radiology, Icahn School of Medicine at Mount Sinai; and the Department of Radiology at Oxford University. Scanning undertaken at the Icahn School of Medicine was performed using a 7T Bruker Biospec MR System. The brains of specimens FC1, PT1, L1, VV1, VZ1, CLL2, CB2, CF2, CF1, LP1, CL1, and D1 were removed within 14 h of death and immersion fixed in 10% formalin at necropsy before being transferred to a solution of 0.1 M phosphate-buffered saline with 0.1% sodium azide solution and stored at 4°C prior to scanning. A 3D fast low angle shot sequence was used with parameter settings of: time to repetition (TR) = 36 ms, time to echo (TE) = 23 ms, flip angle = 15, field of view (FOV) = 128 × 128 × 175, matrix size = 384 × 384 × 384 mm in each slab, 20 averages, slice thickness = 0.5 mm, and 3D isotropic resolution of 0.30 mm. Scanning undertaken at Oxford University was performed using a 7T Bruker Biospec MR System. Following overdose with sodium pentobarbital (200 mg/kg, i.v., the head of animal CL1 (European wolf)) was perfusion fixed in 2 L of 4% paraformaldehyde in 0.1 M phosphate buffer (PB). The brain was then postfixed in 4% paraformaldehyde in 0.1 M PB for 48 h before storage in freezer storage solution. Scanning was performed at the Wellcome Centre for Integrative Neuroimaging, Nuffield Department of Clinical Neurosciences, University of Oxford. The specimen was scanned on a Siemens 7T whole-body scanner

10969861, 2024, 5, Downloaded from https://onlinelibrary.wiley.com/doi/10.1002/cne.25618 by South African Medical Research, Wiley Online Library on [31/07/2024]. See the Terms and Conditions (https://onlinelibrary.wiley.com/terms-and-conditions) on Wiley Online Library for rules of use; OA articles are governed by the applicable Creative Commons License

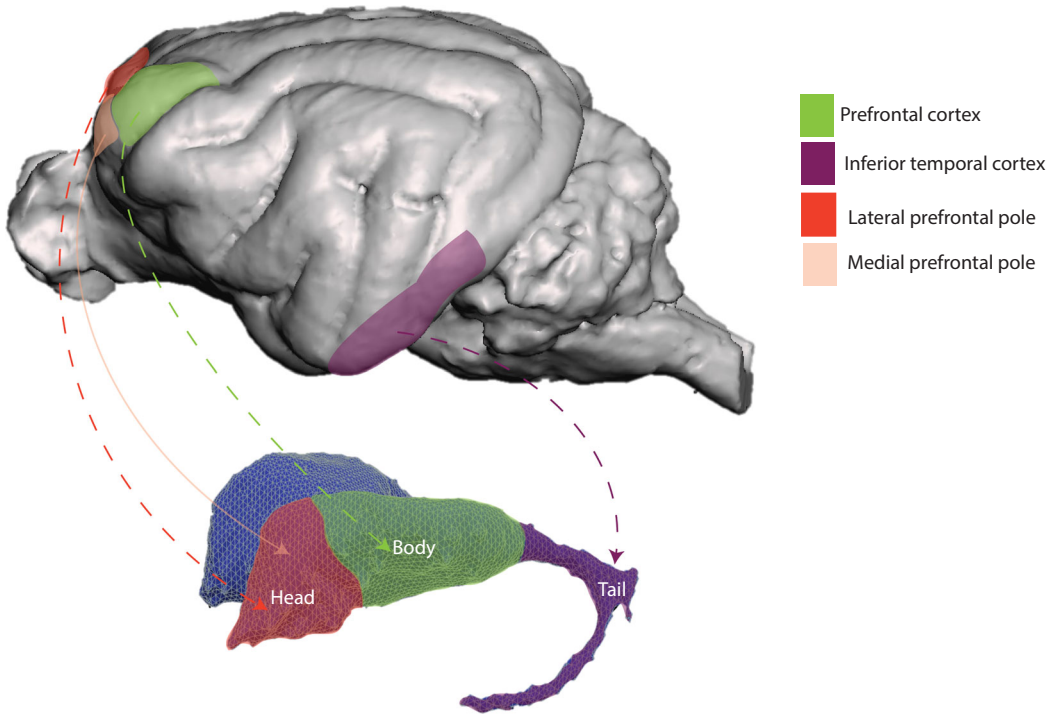

Summary of the connectional relationships derived from Divac, 1972, 1974; Lawicka, 1972; Lawicka, Mishkin & Rosvold, 1975; Frys & Stepien, 1982; Seger & Cincotta, 2005; Yanike & Ferrera, 2014; Grahn et al., 2008; Hikosaka et al., 2000; Villablanca, 2010.

FIGURE 2 An overview of the anatomical subcomponents of the caudate nucleus (caudate head, caudate body, and caudate tail) and their known connection to the cortex along with their general functions. Images were created from 3D reconstruction of the lateral surface of the caudate nucleus and brain of a representative canid species, while the connectional information was summarized from that obtained in Divac (1972, 1974), Frysz and Stepien (1983), Grahn et al. (2008), Hikosaka et al. (2000), Lawicka (1972, 1975), Seger and Cincotta (2005), Villablanca (2010), Yanike and Ferrera (2014). The caudate head is involved in cognition and emotional networks (e.g., evaluating the value of different actions) through its connectional links with the lateral and medial prefrontal pole (dorsal anterior cingulate cortex). The caudate body is functionally involved in perceptual and action-controlling functions (e.g., spatial working memory, inhibitory control, and set-shifting) through its connections to the prefrontal cortex. The caudate tail is involved in processing visual information and the control of movement through connections with the inferior temporal cortex. Lesions of the tail are known to impair the visual discrimination of objects.

(28-channel receive/1-channel-transmit knee coil—QED). A high-resolution structural scan was acquired using a true fast imaging with steady-state free-precession sequence, TR = 14.65 ms, TE = 7.33 ms, flip angle = 30°, FOV = 118 × 160 × 99 mm in each slab, matrix size = 542 × 736 × 448, and 3D isotropic resolution of 0.22 mm.

2.3 | MR image preprocessing and segmentation

Following MR image acquisition, the resulting DICOM files were loaded into Analyze software v. 10.0 (www.analyzedirect.com, RRID:SCR_005988) for postprocessing using a traditional volumetric approach. Traditional volumetry is widely considered the gold standard for volumetric research having been applied on a wide range of populations and anatomical regions and showing both a high degree of reliability and validity (Emerton et al., 2009). Although voxel-based approaches are certainly faster and less reliant on expert/rater guidance to complete tracings, there have been numerous questions raised about the veracity of the assumptions of this approach (Douaud et al., 2006; Juh et al., 2006). In the current study, given the small sample sizes per species, we opted for the use of traditional volumetry as this allowed for the manual tracing of each region of interest and close inspection and validation by the raters.

Before segmentation, MR images were visually inspected to ensure that processing had not inadvertently distorted the hemispheric surface or anatomical midline, affecting the shape of the caudate. The postprocessing steps involved resectioning the image sequences along the A–P plane to facilitate import into ITKSNAP software (http://www.itksnap.org, RRID:SCR_002010). MR images were then loaded into ITKSNAP for caudate segmentation and surface reconstruction. Unless otherwise noted, all caudate volumes were reconstructed for the left hemisphere of each specimen. The ITKSNAP toolkit provides several options for both automatic segmentation (using Region Competition Snakes and Geodesic Active contours) and fully manual segmentation procedures (Yushkevich et al., 2006). Due to the image characteristics, we used manual segmentation procedures to isolate and reconstruct the caudate nucleus (head, body, and tail), while semiautomatic segmentation was used for whole brain volumes. Using the region of

10969861, 2024, 5, Downloaded from https://onlinelibrary.wiley.com/doi/10.1002/cne.25618 by South African Medical Research, Wiley Online Library on [31/07/2024]. See the Terms and Conditions (https://onlinelibrary.wiley.com/terms-and-conditions) on Wiley Online Library for rules of use; OA articles are governed by the applicable Creative Commons License

interest tool, the caudate nucleus was outlined in all coronal slices in which it appeared. The head, body, and tail portions were included to the point where the tail was no longer visible alongside the dorsal surface of the inferior horn of the lateral ventricle.

We parcellated the caudate nucleus into the head and body of the caudate for separate volumetric analyses. Given known connectional and functional differences between the caudate head and body, we hypothesized that the parcellation of the caudate and subsequent analysis would allow us to better identify potential species differences related to the underlying functions of the head and body. The delineation between the head and body of the caudate was performed by using the interventricular foramen as the delineating anatomical landmark (Levitt et al., 2002). In accordance with previous studies, the interventricular foramen was defined as the most posterior coronal slice where any part of the anterior column of the fornix was visible, while the posterior border was defined as the coronal slice appearing just before the atrium (Levitt et al., 2002). Because of difficulties adequately separating the ventral striatum (nucleus accumbens) from the merged putamen and caudate anteriorly, our definition of the head of the caudate nucleus pragmatically includes the nucleus accumbens. Hence, we hypothesize that by our definition, this area is expected to receive its major innervation from the lateral and medial prefrontal cortex and be involved in functions that include the evaluation of different action value as well as stimulus motivation. Segmentation outlines were completed by MF and MAS and visually inspected by both investigators for consistency through reference to relevant anatomical atlases on canine and human brains (e.g., Mai et al., 2015; Palazzi, 2011). Associated whole brain volumes were also segmented for each specimen using semiautomatic segmentation as applied through the Region Competition Snake algorithm. To validate our approach, a pilot study was conducted on two randomly selected brain scans (one canid and one felid) by two observers (MF and MAS). Each observer was responsible for independently segmenting the caudate nucleus with interobserver congruency assessed (Lin, 1989). Despite variability in the most caudal extent of the caudate tail, high congruencies in volume measures were obtained by the two observers (i.e., Lin's concordance >90%), suggesting that the caudate delineations were highly reproducible. An overview of the parcellation and segmentation procedure is provided in Figure 3. The resultant 3D reconstructions were then saved as stereolithographic files before being imported into the open-source mesh editing software MeshLab (http://www.meshlab.net/, RRID:SCR_003430) for further analysis (i.e., curvature and cross-sectional strength analysis). Volumetric and surface area data from each species were then computed in MeshLab before being tabulated in Microsoft Excel in preparation for statistical analysis in R.

2.4 | Curvature analysis

3D anatomical modeling of the caudate surface can provide additional information on the spatial properties of the caudate not reflected in the size of the structure. We used shape-based techniques (applied through the imaging pipeline of MeshLab) as a means of visually comparing the 3D anatomical surface of the caudate in each species. We computed Gaussian curvatures for each resulting caudate mesh in MeshLab. Curvature analyses have been conducted on earlier studies of the human cortical surface (e.g., Batchelor et al., 2002; Pienaar et al., 2008; Shimony et al., 2016), and here we applied them to the study of carnivore brains. Curvature is a scalar quantity that provides a measure for the amount of bending at a point on a convoluted surface (Demirci & Holland, 2022). The Gaussian curvature is considered an invariant measure (unless the surface is distorted through shearing or stretching) of intrinsic bending/distortion (Chiek, 2006). This measure has been used in earlier studies of mammalian brains to compare cortico–cortico connectional lengths (Ronan et al., 2011, 2014). Use of this metric to analyze the caudate reflects intrinsic bending forces resulting from aspects of normal biological growth. Using MeshLab, 3D mesh files of the caudate nucleus were subjected to curvature analysis using the modeling modules in MeshLab (Figure 4). The initial process involved smoothing through the application of two smoothing filters. First, we applied Laplacian smoothing (parameters: smoothing steps = 3; 1D boundary smoothing; contingent weighting) followed by face normal smoothing. We then applied the Curvature Calculation Filter to compute the Curvature Principal Directions and used Principal Component Analysis to map the mesh quality to the Gaussian curvature data. Each mesh was then rendered and visually compared for areas of high curvature (hot colors) versus low curvature (cool colors). Along with curvature data, we also extracted surface area and volume data using the Quality Measures and Computation Module and computed the linear dimensions of the caudate nuclei using Meshmixer (analysis module; submodule: units/dimensions; see Figure 4). Although a notable challenge to our models is the limited sample size for each species, we believe that these maps provide valuable comparative data to evaluate interspecific differences in caudate surface morphology.

2.5 | Cross-sectional structural analysis

In addition to the computation of curvature data, we also used cross-sectional structural analysis as applied in MeshLab to calculate the relative strength of each mesh and mapped this strength data back onto the 3D space of the caudate (head, body, and tail) to provide a heat map showing areas of weakness and relative strength (Figure 4). This technique detects critical stress inside a 3D object. The object is partitioned into cross sections, and the critical stress is computed at each section based on the bending momentum equilibrium. The results of these analyses are displayed in MeshLab as a heat map with hot colors indicating areas of maximum weakness, while cooler areas are sites of minimum weakness (i.e., less likely to fracture under stress). This procedure as applied in MeshLab uses the Euler–Bernoulli assumption to focus on the geometric relationship between a cross section and external loads (Autodesk, 2010). As a consequence, this procedure ignores deformation outside the cross section and specifically points to weak parts of the 3D object (Autodesk, 2010).

10969861, 2024, 5, Downloaded from https://onlinelibrary.wiley.com/doi/10.1002/cne.25618 by South African Medical Research, Wiley Online Library on [31/07/2024]. See the Terms and Conditions (https://onlinelibrary.wiley.com/terms-and-conditions) on Wiley Online Library for rules of use; OA articles are governed by the applicable Creative Commons License

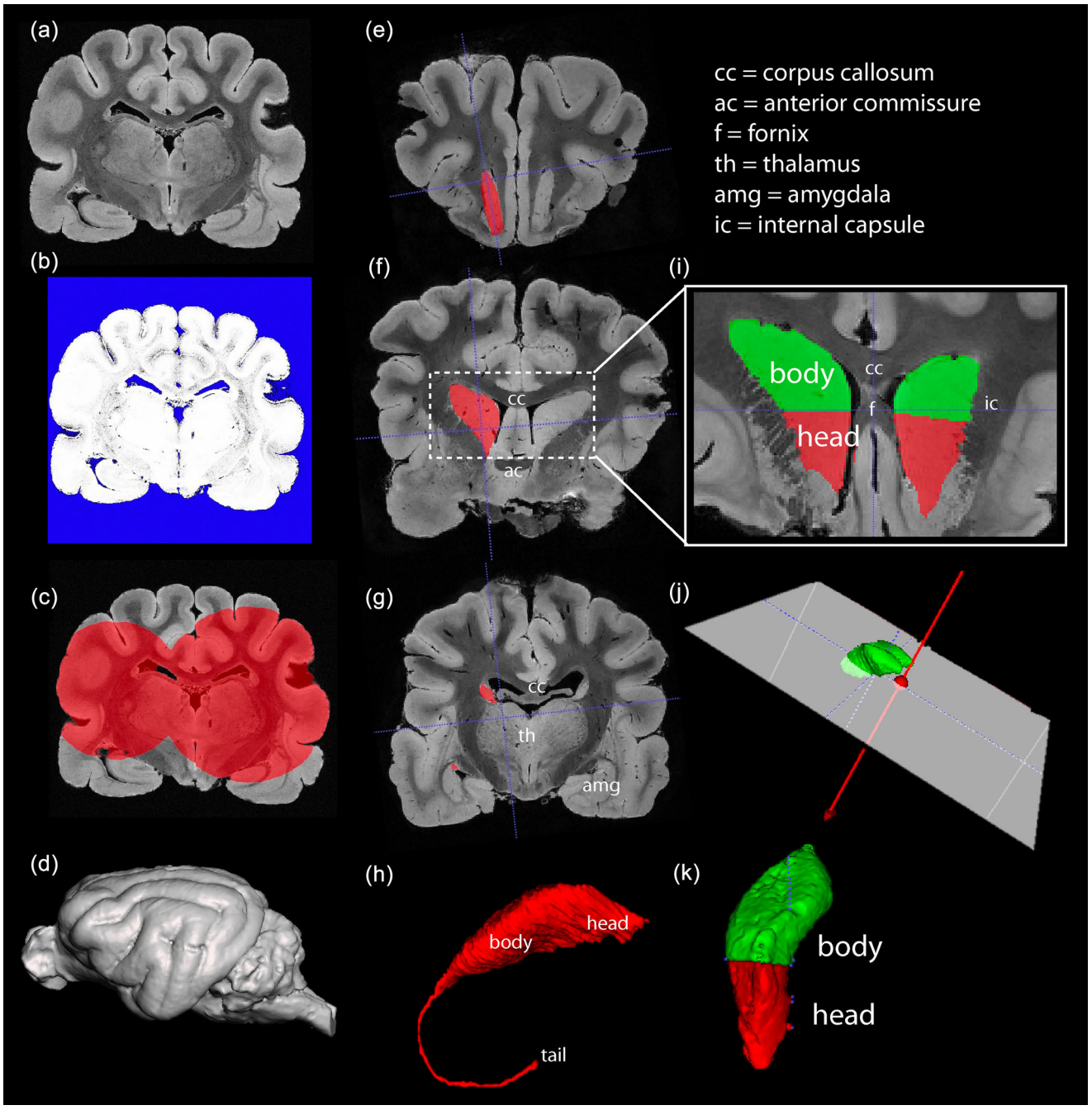

FIGURE 3 A summary of the segmentation pipeline used in ITKSNAP for semiautomatic segmentation of the whole brain (a–d) and manual segmentation of the caudate nucleus (e–k). (a) Representative MR coronal image through the diencephalon of a felid (*Felis silvestris catus*); (b and c) screenshots of the active contour segmentation process using the speed function and guided by user placed initialization seeds; (d) a representative screenshot of a completed 3D surface reconstruction of the felid brain using semiautomatic segmentation. (e–g) Representative coronal images through the caudate head, body, and tail; (h) a 3D reconstruction of the caudate nucleus completed through manual segmentation; (i–k) representative screenshots showing the parcellation of the caudate head and body. The parcellation landmarks are described in detail in Section 2.

2.6 | Data analysis

We used phylogenetic generalized least squares (PGLS) regression analysis to evaluate the scaling attributes of the caudate nucleus (i.e., whole volume, caudate head, and caudate body) against brain volume. All statistical analyses were undertaken in R v. 3.4.1 (www.r-project.org/ with PGLS being performed using the "caper" add-on package) (Orme et al., 2013). The phylogeny used in the current study is shown in Figure 1 as derived from Bininda-Emonds et al. (2007, 2008), Nyakatura and Bininda-Emonds (2012). Note that the data points for the domestic dogs (*C. lupus familiaris*) and dingo (*C. lupus dingo*) were not included in the regressions but were superimposed on the regression

10969861, 2024, 5, Downloaded from https://onlinelibrary.wiley.com/doi/10.1002/cne.25618 by South African Medical Research, Wiley Online Library on [31/07/2024]. See the Terms and Conditions (https://onlinelibrary.wiley.com/terms-and-conditions) on Wiley Online Library for rules of use; OA articles are governed by the applicable Creative Commons License

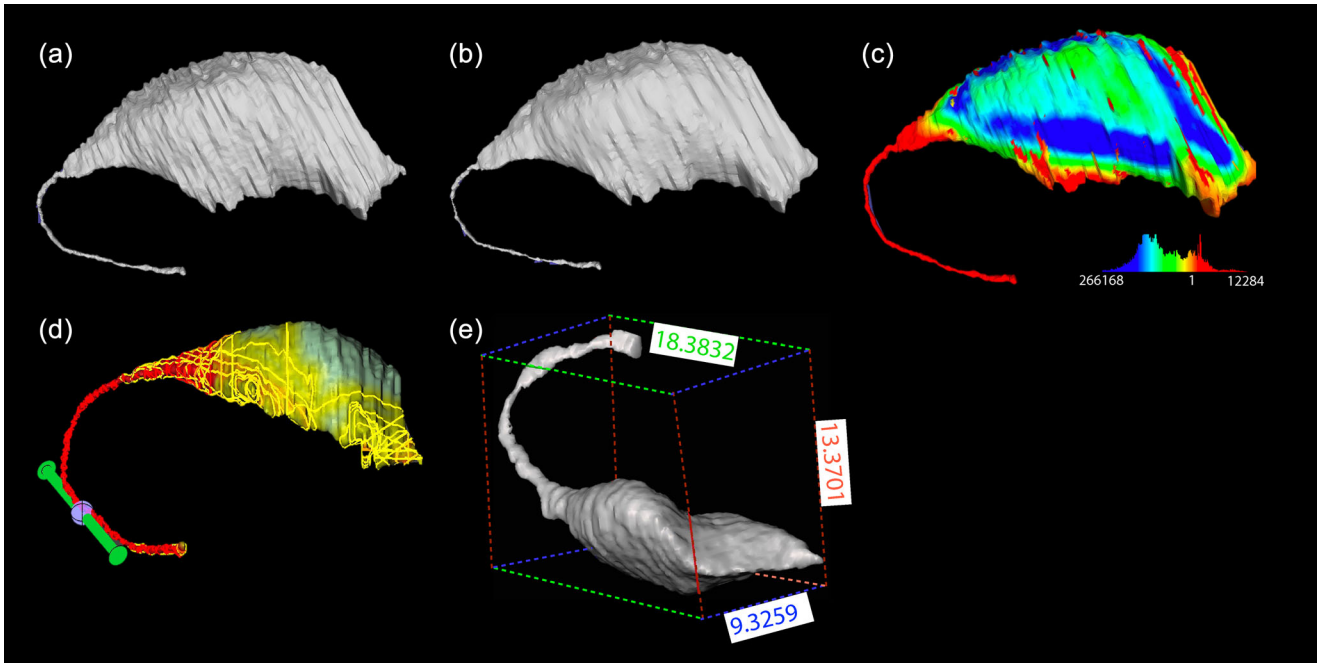

FIGURE 4 Sample images showing the process used in computing curvature maps of the caudate nucleus (a–e) as well as cross-sectional structural analysis in MeshLab. (a) A representative image of the caudate nucleus showing the raw/unprocessed 3D mesh file generated in ITKSNAP through manual segmentation; (b) resultant mesh file after initial smoothing in MeshLab through the application of Laplacian and face normal smoothing; (c) an example of a resultant Gaussian curvature map with curvature data mapped back onto the vertex quality data; (d) an example of the strength data obtained from cross-sectional analyses of the caudate mapped back onto the 3D surface; (e) a representative image showing volumetric and linear dimensions obtained from caudate mesh file using the MeshLab.

TABLE 2 Summary of the regression statistics for caudate volume and its subcomponents scaled against brain volume, species group size, and species home range.

Model (*x* variable; *y* variable)	λ	Adjusted R^2	Slope	SE	*t*-Value	*p*	Intercept	SE
PGLS (brain volume, whole caudate volume)	.73	.99	.8	.02	33.52	5.45×10^{-9}	−1.45	.05
PGLS (brain volume, caudate head volume)	0	.88	.89	.11	7.88	0	−2.59	.21
PGLS (brain volume, caudate body volume)	0	.92	.71	.07	9.66	2.68×10^{-5}	−1.76	.14
PGLS (caudate head volume, species group size)	0	−.06	.25	.35	.72	.50	−1.07	.18
PGLS (caudate body volume, home range)	0	.79	2.63	.50	5.25	.00	2.52	.26
PGLS (residuals caudate head volume—brain volume, species group size)	0	.03	.57	1.20	.47	.65	.40	.12
PGLS (residuals caudate head volume—brain volume, home range)	0	.11	3.72	3.98	.93	.38	1.32	.27

Note: All regression statistics were obtained using phylogenetic generalized least squares regression (PGLS). PGLS was performed using Caper (Orme et al., 2013).

lines to evaluate their relative placement. The raw data used to derive these relationships are shown in Table 1, and a summary of the regression statistics derived from the analyses is shown in Table 2. In addition to comparing the scaling attributes of the caudate to brain mass, we also evaluated scaling attributes of the caudate head and caudate body to published average species group size and home range. Species values for each of these estimates were sourced from Michaud et al. (2022). To account for the likely effect of brain size in our comparisons, we computed the residuals of caudate head and body size against brain volume and regressed these residuals against species group size and home range, respectively.

2.7 | Limitations

One of the limitations of the current study is the small sample sizes available to adequately address questions concerning the range of intraspecific variation within each species. This is a common

10969861, 2024, 5, Downloaded from https://onlinelibrary.wiley.com/doi/10.1002/cne.25618 by South African Medical Research, Wiley Online Library on [31/07/2024]. See the Terms and Conditions (https://onlinelibrary.wiley.com/terms-and-conditions) on Wiley Online Library for rules of use; OA articles are governed by the applicable Creative Commons License

limitation of comparative studies, especially those using charismatic species which are difficult to acquire. Given this limitation, we focused our attention on the interspecific patterns in caudate morphology which provide us with an opportunity to characterize changes in volumetry as it relates to brain size. Although we acknowledge that intraindividual variation in age, sex, reproductive status, and life history can impact brain volumetry, we feel that our approach focused on species-level differences in a cross species analysis, as undertaken here, is appropriate given the limitations and helps characterize species typical patterns in caudate morphology which differentiate the group.

It is also important to note that our interpretations on the connectivity, behavioral, and cognitive functions of the head and tail of the caudate, as presented here, are largely extrapolated from the extensive primate and rodent literature on the topic. Direct observations have only been completed in a limited manner on a small subset of domestic and wild Carnivora (Cook & Berns, 2022). Although we acknowledge this caveat, and that the Euarchontoglires have been separated from the Carnivora by almost 90 million years of evolution, we argue that evidence of strong conservation of the morphological plan as exemplified by scaling analyses of the cortical and subcortical structures (e.g., Bush & Allman, 2004) suggests that certain shared characteristics underlie the connectivity and function of the caudate and its subcomponents.

3 | RESULTS

3.1 | Scaling of the caudate nucleus with brain volume, species group size, and home range

Regression analysis (PGLS) revealed a strong positive relationship between the size of the whole caudate nucleus and brain volume (PGLS slope = .80, $p = 5.45 \times 10^{-9}$, R-squared = .99) (Figure 8a; Table 2), indicating that 99% of the variance in caudate volume could be explained by brain size. The lambda value for the regression line indicated the presence of a phylogenetic signal in the data (i.e., $\lambda = .73$); thus, phylogenetic correction was warranted (Table 2). Although all species data points were well within the prediction intervals, the data points for the domestic dog (*C. lupus familiaris*) lay outside of the confidence intervals and close to the upper bound for the prediction intervals.

Caudate head volume regressed against brain volume displayed strong positive allometric scaling (PGLS slope = .89, p = .00, R-squared = .89, $\lambda = 0$) (Figure 8b) with 88% of the variance in the size of the caudate head being attributed to brain size. Although the majority of the species data points were within the prediction intervals, the data points for the coyote (*C. latrans*), the domestic dog (*C. lupus familiaris*), and dingo (*C. lupus dingo*) were found to lie outside of the confidence interval.

Similarly, regression analysis of caudate body size plotted against brain volume revealed allometric scaling (PGLS slope = .71, $p = 2.68 \times 10^{-5}$, R-squared = .92, $\lambda = 0$) (Figure 8c) with approximately 92% of the variance in the size of the caudate body being explained by variance in brain size. All species data points were within the prediction intervals, but the European wolf (*C. lupus lupus*) and tiger (*P. tigris*) had data points that were found to lie slightly outside of the confidence intervals.

Regression analysis of caudate head volume regressed against species group size revealed no significant relationship between the two variables (PGLS slope = .25, p = .50, R-squared = .07, λ = .00). Similarly, scaling analysis of the residuals of caudate head volume and brain volume regressed against species social group size also revealed no significant relationship (PGLS slope = .57, p = .65, R-squared = .03, $\lambda = 0$) (Figure 9a), with only 3% of the variance in size of the caudate head attributed to the variance in group size. In contrast, caudate body size was found to be significantly, positively correlated with home range with 79% of the variance in the caudate body being explained by variance in home range size (PGLS slope = 2.63, p = .00, R-squared = .79, $\lambda = 0$) (Figure 9b); however, when correcting for brain size by regressing the residuals of caudate body size and brain volume against home range, we found that home range was not significantly correlated with caudate body size residuals (PGLS slope = 3.72, p = .38, R-squared = .11, $\lambda = 0$). Although all species data points were within the prediction intervals for this regression, the African wild dog (*L. pictus*) data point was found to lie slightly outside of the confidence interval and nearer the upper bound for the prediction intervals (Figure 9).

3.2 | Shape analysis and cross-sectional properties of the caudate nucleus

To test for shape differences in caudate morphology in our sample, we computed Gaussian curvature profiles and visually compared the curvature heat maps between canids and felids. As shown in Figures 5 and 6, despite wide differences in brain size and shape, there appeared to be consistency in curvature maps between these clades. As exemplified in the comparison of curvature profiles for the domestic cat (*F. silvestris catus*) and the tiger (*P. tigris*) (Figure 5), marked curvature in the heat maps of the lateral and medial surfaces of the caudate was observed with areas of low curvature near the body of the caudate and areas of high curvature near the ventral body and tail of the caudate. This pattern of curvature was also consistent with that observed in the snow leopard (*P. uncia*). Similarly, we observed fairly consistent patterning of curvature across these canids with areas of low curvature along the medial and lateral surface of the caudate body (i.e., cooler colors) and areas of high curvature near in the ventral body and tail of the caudate. One notable difference among the canids' curvature maps was the observation of a consistent area of high curvature in the rostral surface of the caudate in domestic dogs (*C. lupus familiaris*), an observation that was also slightly evident in the rostral surface of the coyote (*C. latrans*).

We also applied cross-sectional structural analysis to each mesh to calculate its relative strength and mapped this strength data back onto the 3D space to visually compare areas of weakness and relative strength in each mesh (Figure 7). Heat maps of critical stress revealed a consistent point of marked weakness in the caudal body and tail of the caudate nucleus (i.e., hot colors indicate areas of maximum

10969861, 2024, 5, Downloaded from https://onlinelibrary.wiley.com/doi/10.1002/cne.25618 by South African Medical Research, Wiley Online Library on [31/07/2024]. See the Terms and Conditions (https://onlinelibrary.wiley.com/terms-and-conditions) on Wiley Online Library for rules of use; OA articles are governed by the applicable Creative Commons License

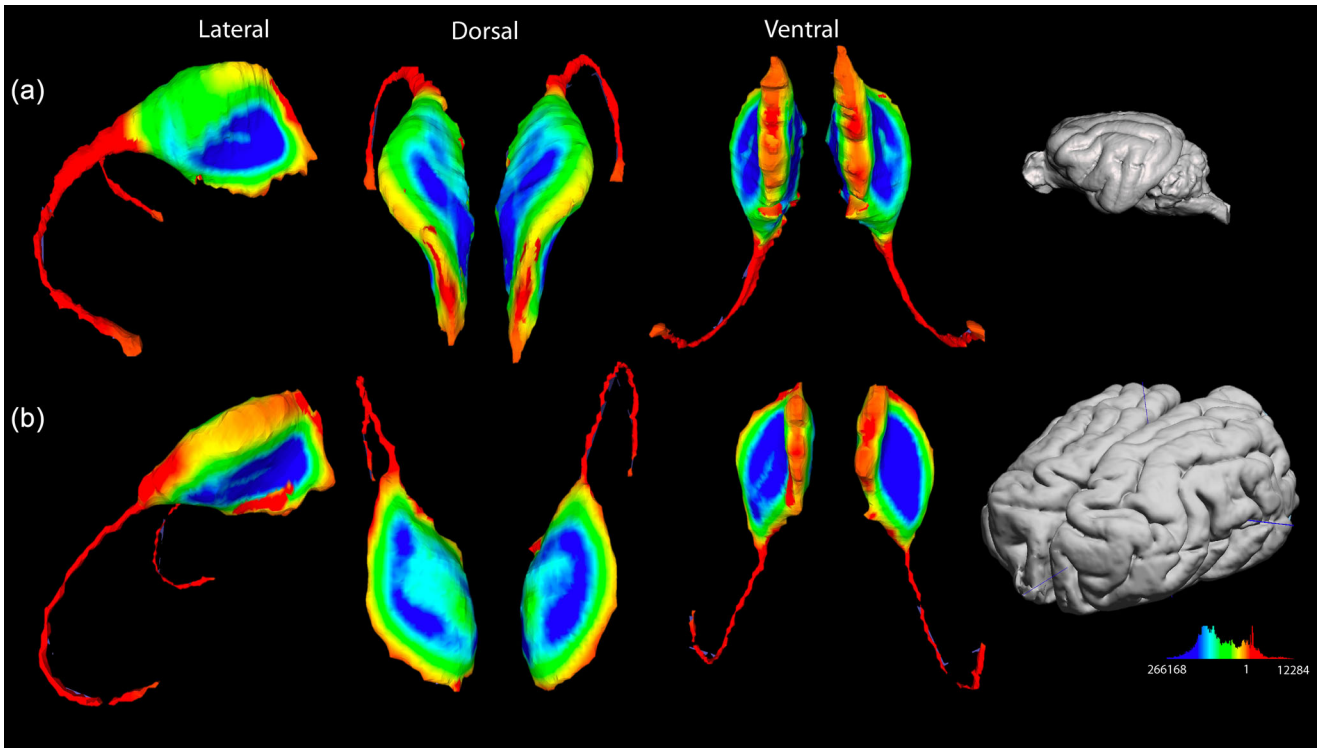

FIGURE 5 Bilateral curvature maps of the caudate nucleus in the domestic cat (a) and Siberian tiger (b). Note the marked similarity in heat maps of the lateral and medial surface with areas of low curvature near the body of the caudate and areas of high curvature in the rostral body and tail of the caudate. These similarities in curvature are notable when considering the marked differences in brain shape and size between these two species [i.e., the tiger brain (231.24 g) is nine times bigger than the cat brain (25.39 g) and more dorsoventrally compressed]. Areas of high curvature are shown in the warm colors, while cooler colors indicate lower curvatures.

weakness, while cooler areas are sites of minimum weakness and less likely to fracture) across canids and felids. Despite this consistency, we also noted that the caudate nucleus of the fennec fox (*V. zerda*) was a clear outlier in the group as it had large areas of maximum weakness/fracture extending into the caudate midbody and head area. This relative extension of the fracture points into the mid caudate body was also observed in the domestic cat albeit to a much lesser extent.

4 | DISCUSSION

Scaling analyses revealed that brain size is a strong predictor of caudate size across the Canidae and Felidae. Similar results were obtained for scaling analyses of the caudate head and caudate body. Although all species data points lay within the prediction intervals of the regressions, we observed some notable deviations. The domestic dog data were consistently found close to the upper bound for the prediction intervals of whole caudate nucleus and caudate head size versus brain size. We tested for a relationship between the sizes of the head of the caudate with social group size and found no significant association. The body of the caudate was positively and strongly correlated with home range size but not after correcting for brain size. Apart from a slight deviation in the rostral caudate of the domestic dog, curvature analyses revealed an overall consistent pattern of curvature across canid and felid species. Similar patterns of consistency in caudate fracture points were obtained from cross-sectional structural analysis, with the only notable exceptions being an extension of the fracture areas into the midbody and head of the caudate for the fennec fox and domestic cat.

4.1 | Scaling of the caudate nucleus with brain mass, species group size, and home range

In accordance with previous observations of scaling in the mammalian brain (Manger et al., 2013), we observed a strong pattern of positive hypoallometric (i.e., slope <1) change in caudate size with increases in brain size, indicating that the rate of the caudate volume increase is lower than that of brain volume. This linked regularity in scaling across species was also observed for the head of the caudate nucleus, as well as the body of the caudate, although the scaling relationships for the body were characterized by a hyperallometric pattern (i.e., >1.0) such that caudate body volume increase is higher than that of increases in brain size. A combination of genetic (Onorati et al., 2014) and developmental control (Deacon et al., 1994) paired with the potential for developmental plasticity through adult neurogenesis (Dayer

10969861, 2024, 5, Downloaded from https://onlinelibrary.wiley.com/doi/10.1002/cne.25618 by South African Medical Research, Wiley Online Library on [31/07/2024]. See the Terms and Conditions (https://onlinelibrary.wiley.com/terms-and-conditions) on Wiley Online Library for rules of use; OA articles are governed by the applicable Creative Commons License

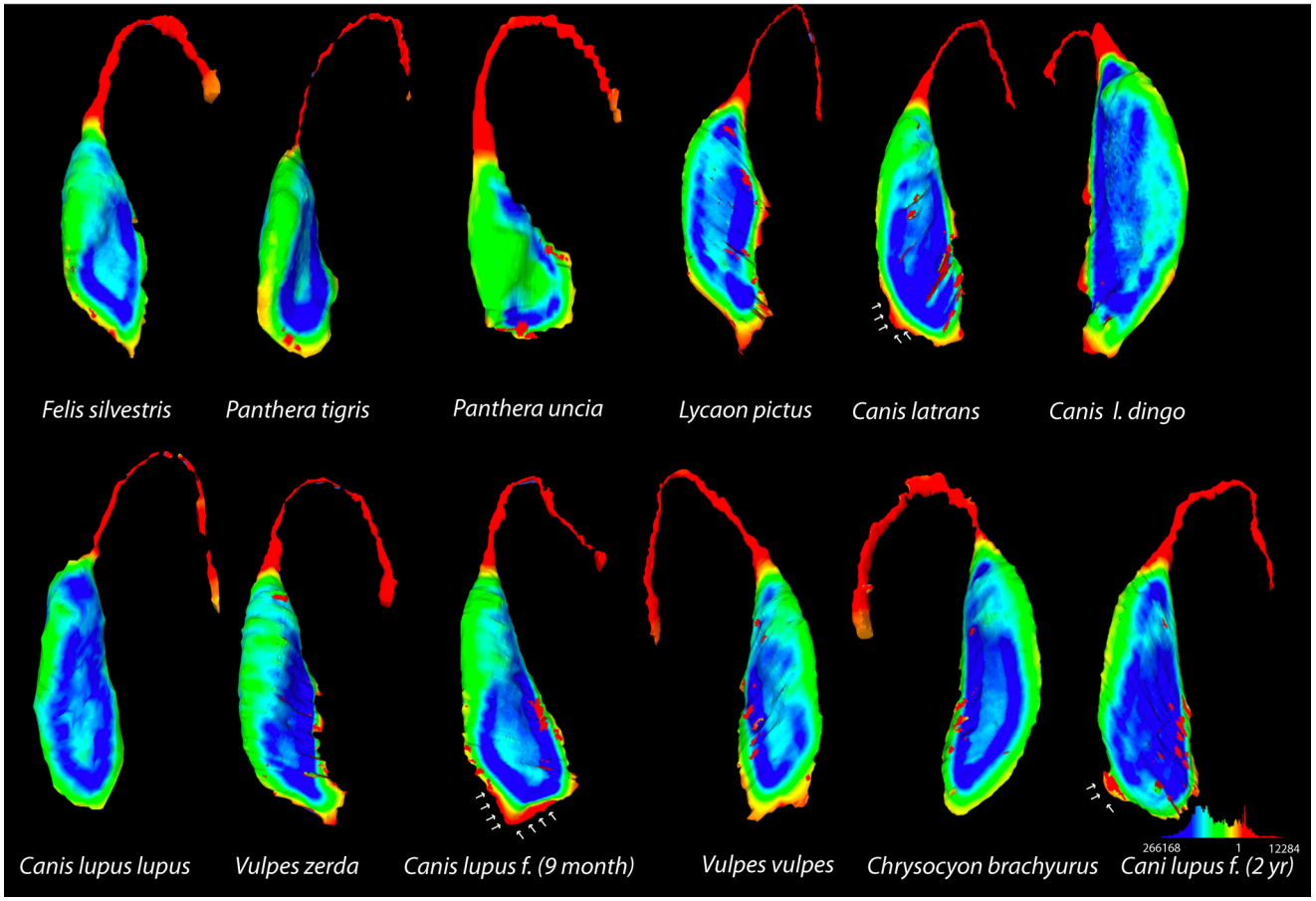

FIGURE 6 Gaussian curvature maps of the lateral surface of the caudate nucleus in 12 carnivore specimens. Areas of high curvature are shown in the warm colors, while cooler colors indicate lower curvatures. The caudate sizes have been normalized to facilitate visual comparison. In some cases, the right caudate was substituted for the left due to challenges with the resultant segmentation. Note the marked areas of high curvature (warm colors) in the head of the caudate nucleus in the domestic dog (*Canis lupus familiaris*) also present to a lesser extent in the coyote (*Canis latrans*).

et al., 2005; Ernst et al., 2014; Luzati et al., 2006) or the impact of environmental factors (see Isaacs et al., 2008) may, in part, be responsible for the close alignment in interspecific scaling attributes observed for the caudate nucleus. Although our analyses demonstrated these scaling relationships, we also observed a notable deviation in the scaling of the caudate nucleus for the domestic dog. To the best of our knowledge, only one other study has quantitatively compared caudate volume in wild Carnivora (Cook & Berns, 2022). These authors provide volumetric measures for the caudate and putamen volume in two coyotes and two California sea lions. These published volumes are in strong alignment with that presented in the current study albeit slightly smaller (0.88 vs. 1.21 g) as the authors notably did not include the caudate tail in their segmentations (Cooks & Berns, 2022).

In recent years, studies on the behavior of domestic dogs have revealed a suite of convergent socio-cognitive skills (e.g., Bräuer et al., 2006; Hare & Tomasello, 2005; Hare et al., 1998; McKinley & Sambrook, 2000; Miklösi et al., 1998) that may have been shaped through the domestication process (Hare et al., 1998). Although comparative neuroanatomical data on domestic dogs compared to other canids are limited, dogs are known to: (1) have undergone a reduction in overall brain size relative to wild-type canids (Röhrs & Ebinger, 1978); (2) have increased variability in brain size (Kruska, 1980; Schleifenbaum, 1973); (3) have increased variation in corpus callosum morphology and an extension of the rostral component of the corpus callosum (Spocter et al., 2018); (4) have a putative larger number of cortical neurons (Jardim-Messeder et al., 2017); and (5) have increased variability in cortical gyrification and a reduction in gyrification of the visual cortex (Grewal et al., 2020), as well as breed specific patterning of connectivity (Hecht et al., 2019). Of particular relevance to the current study, Berns et al. (2012, 2013) used fMRI in fully awake dogs to evaluate brain activation in the caudate nucleus (focused on the head of the caudate) using the contrasts of reward versus no reward hand signals. These results revealed significant activation in the caudate nucleus when dogs were presented with associated hand signals and food reward, a pattern that the authors note was strikingly similar to caudate activation observed in humans and nonhuman primates (Berns et al., 2012, 2013). Furthermore, the canine medial caudate was also activated when animals were presented with familiar versus unfamiliar human and other conspecific odors (Berns et al., 2015). An interesting observation from this study was that although the olfactory bulbs

10969861, 2024, 5, Downloaded from https://onlinelibrary.wiley.com/doi/10.1002/cne.25618 by South African Medical Research, Wiley Online Library on [31/07/2024]. See the Terms and Conditions (https://onlinelibrary.wiley.com/terms-and-conditions) on Wiley Online Library for rules of use; OA articles are governed by the applicable Creative Commons License

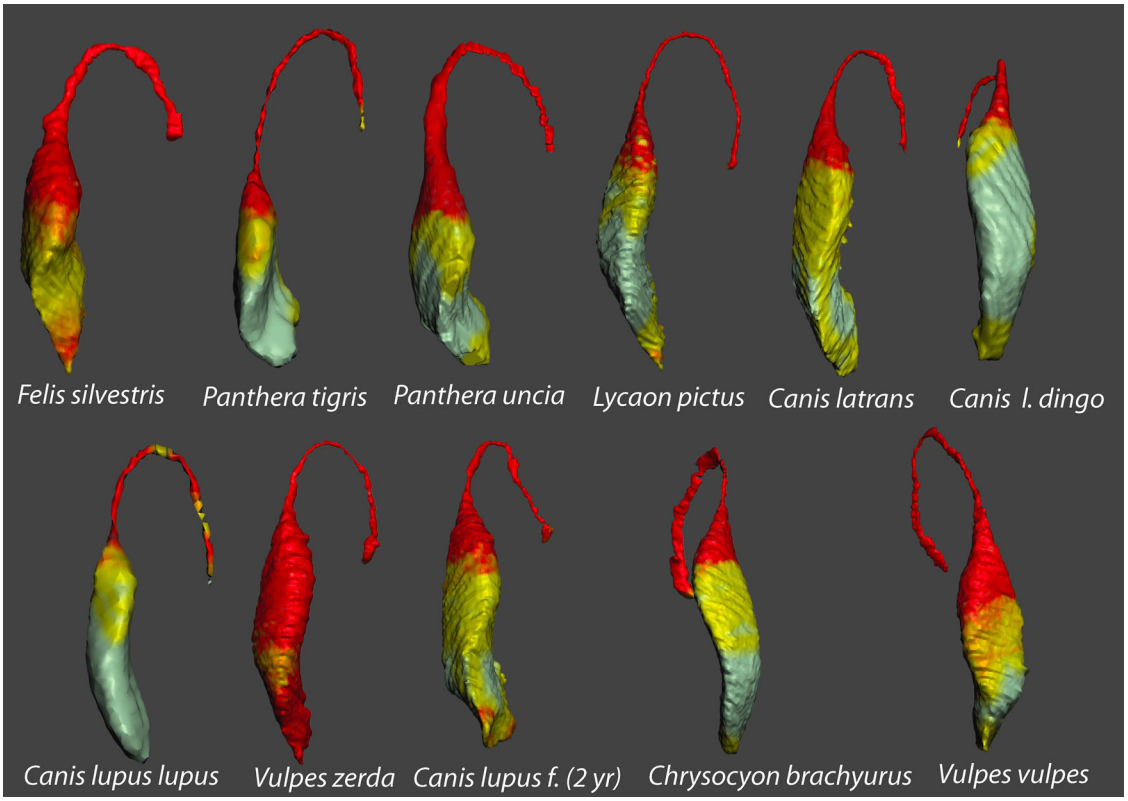

FIGURE 7 Results of cross-sectional structural analyses obtained in MeshLab for each mesh in 12 carnivore specimens. This technique detects critical stress inside a 3D object. The object is partitioned into cross sections, and the strength is computed at each section based on the bending momentum equilibrium. Hot colors indicate areas of maximum weakness, while cooler areas are sites of minimum weakness and less likely to fracture. Note the marked weakness in the rostral body and tail of the caudate across species. Also note that the fennec fox (*Vulpes zerda*) and domestic cat (*Felis silvestris catus*) were the smallest of all the Carnivora in this sample and appeared to have expanded areas of maximum weakness/fracture extending into the mid caudate body and head.

were activated by all scents, caudate activation peaked with the presentation of the familiar human, indicating that the dogs were able to discriminate familiar versus unfamiliar scents (Berns et al., 2015). The role of the caudate nucleus in evaluating different actions and making associations and predictions with positive expectations has been studied extensively in humans (e.g., Izuma et al., 2008; Montague & Berns, 2002; Rilling et al., 2002), nonhuman primates (e.g., Doi et al., 2020; Schultz et al., 1997), and rodents (e.g., Knutson et al., 2001). The caudate receives inputs from the cerebral cortex in the form of glutamatergic neurons as well as modulatory dopaminergic inputs (Koob, 1992; Matz & Spocter, 2022). This dopaminergic input is believed to signal rewarding stimuli in the caudate (Daw et al., 2011; Schultz et al., 1997). Lesion studies have revealed that injuries to the anterior caudate are associated with disturbances in the reward pathway as well as in the processing of feedback during associative learning (e.g., Yanike & Ferrera, 2014). These studies have revealed that the anterior aspect of the caudate simultaneously encodes spatial, risk, and reward information as it is sent to the frontal cortex (Yanike & Ferrera, 2014). In contrast, the caudate body and tail are involved in the acquisition of learning associations between stimuli and responses/categories (Seger & Cincotta, 2005). The discovery that damage to the anterior caudate nucleus in monkeys resulted in behavioral impairments similar to those found after prefrontal lesions, stimulated research into the functional role of the caudate nucleus and its functional links to the prefrontal cortex. Early lesion studies in monkeys showed that lesions of the tail of caudate impaired visual discrimination (Divac et al., 1967) and that the caudate tail received projections from the inferotemporal cortex (Mishkin & Pribram, 1954). Further studies in monkeys revealed that the head of the caudate nucleus receives projections from the frontal cortex and that lesions in the ventrolateral head of the caudate resulted in impaired performance on object reversal tasks, while lesions of the anterior dorsal head of the caudate nucleus resulted in impairments in spatial alternation tasks (Pribram et al., 1952). These results were later extended to domestic felids (*F. silvestris catus*) (Divac, 1972, 1974), demonstrating that lesions of both the prefrontal cortex and head of the caudate nucleus impaired performance on a delayed alternation task. Problems of spatial discontiguity have been investigated in monkeys (Goldman & Rosvold, 1970; Podbros et al., 1980) and dogs (Lawicka, 1972, 1975; Stepien et al., 1966, 1975) following prefrontal lesions. These studies were concerned with an animal-orienting response in spatial requirements (e.g., Lawicka et al., 1975), and the impairment caused by either prefrontal or anterior caudate lesions (Potegal, 1972). Subsequent study in domestic cats revealed that the head of the caudate (especially its

10969861, 2024, 5, Downloaded from https://onlinelibrary.wiley.com/doi/10.1002/cne.25618 by South African Medical Research, Wiley Online Library on [31/07/2024]. See the Terms and Conditions (https://onlinelibrary.wiley.com/terms-and-conditions) on Wiley Online Library for rules of use; OA articles are governed by the applicable Creative Commons License

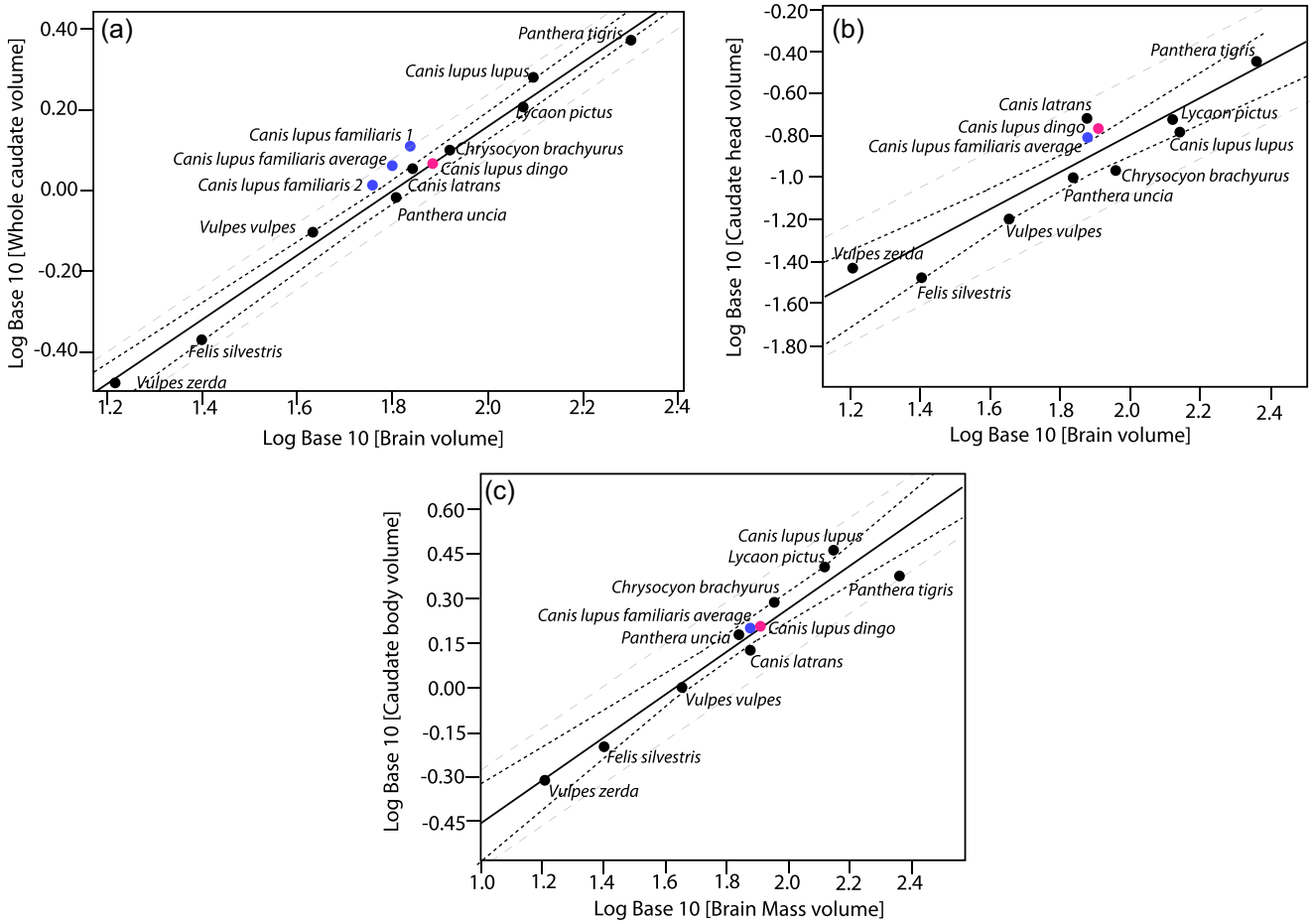

FIGURE 8 Plots derived from phylogenetic generalized least squares regression (PGLS) analysis of (a), brain volume plotted against whole caudate volume for the prefrontal cortex; (b) brain volume plotted against caudate head volume, (c) brain volume plotted against caudate body volume. Note that the domestic dog (*Canis lupus familiaris*) and dingo (*Canis lupus dingo*) were not included in the regression analyses but their data points were simply superimposed on the regressions for visual comparison. All data were logarithmically transformed (base 10) prior to inclusion in the regression analyses. Data used to derive these relationships are shown in Table 1. Dotted lines indicate the prediction and confidence intervals for each regression line.

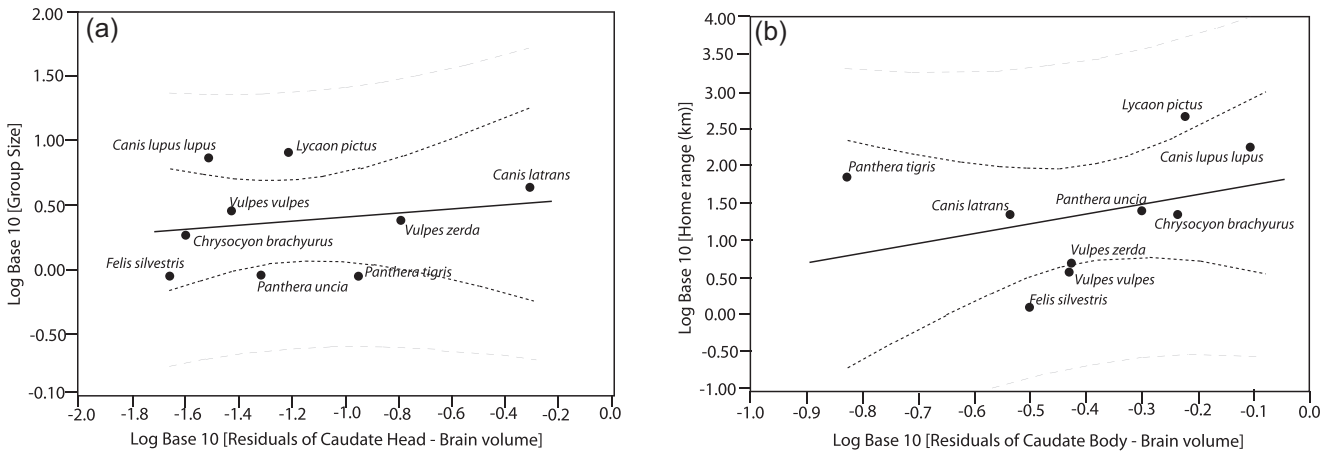

FIGURE 9 Plots derived from phylogenetic generalized least squares regression (PGLS) analysis of (a), residuals of caudate head volume and brain volume plotted against species group size; (b) caudate body volume plotted against home range. All data were logarithmically transformed (base 10) prior to inclusion in the regression analyses. Dotted lines indicate the prediction and confidence intervals for each regression line.

10969861, 2024, 5, Downloaded from https://onlinelibrary.wiley.com/doi/10.1002/cne.25618 by South African Medical Research, Wiley Online Library on [31/07/2024]. See the Terms and Conditions (https://onlinelibrary.wiley.com/terms-and-conditions) on Wiley Online Library for rules of use; OA articles are governed by the applicable Creative Commons License

ventral segment) played an important role in the solution of these tasks, and that lesions of the caudate head resulted in impaired spatial task performance (Frysz & Stepien, 1983). In humans, the medial aspect of the caudate nucleus has been implicated in goal-directed behavior and motivation as well as behavioral flexibility (Grahn et al., 2008; Hikosaka et al., 2000). These observations have also been supported by lesion studies in domestic felids where bilateral damage to the caudate is known to result in hyperactive and compulsive behaviors (Villablanca, 2010). It is notable that these hyperactive and compulsive behaviors in domestic felids functionally parallel the behaviors observed in human obsessive-compulsive disorder, autism spectrum disorder, and attention deficit hyperactivity disorder where caudate dysfunction is known to result in abnormal activation of the thalamus and frontal lobe (Hynd et al., 1993; Lou et al., 1989; Robinson et al., 1995; Scarone et al., 1992; Sears et al., 1999; Sheppard et al., 1999). Studies on domestic felids have also reinforced observations of the caudate involvement in mnemonic function (White, 2009) and demonstrated that large caudate lesions impaired both initial learning and performance on various alternation tasks (Olmstead et al., 1976, Olmstead & Villablanca, 1979; Villablanca et al., 1978). Although we know very little about the connectivity of the caudate in wild Carnivora, a recent study has provided some valuable insight through the use of probabilistic tract tracing in coyotes and California sea lions (Cook & Berns, 2022). This study revealed that both sea lions and coyotes had three primary frontal projections emerging from the caudate: (1) a putative motor cortex projection projecting to the cruciate sulcus, (2) a projection to the premotor and frontopolar cortex heading toward the presylvian sulcus, and (3) an orbitofrontal cortex projection heading toward the orbital gyrus (Cook & Berns, 2022). Collectively, these observations suggest that the caudate is functionally similar to analogous regions in the primate and rodent model (also see Christie et al., 2008).

We hypothesize that our observation of relative increase in caudate volume in domestic dog reflects changes that support error prediction and the evaluation of different actions. In the absence of comparative fMRI studies on caudate activation in wild canids and felids, we postulate that this trait may be a result of the domestication process, facilitating a slight deviation from the constraints of scaling laws of form.

Given the connectional and functional differences between the caudate head and body (Grahn et al., 2008; Hikosaka et al., 2000; Lawrence et al., 1998; Middleton & Stick, 1996; Seger & Cincotta, 2005; Yanike & Ferrera, 2014), we analyzed the scaling of these individual components with brain size (as well as select ecological variables). The domestic dog, dingo, and coyote were found to have relatively larger than expected caudate head sizes. These observations in the dog are consistent with our hypothesis that the canine caudate has undergone volumetric changes to support the function of error prediction and action evaluation as a result of domestication. Similarly, observations in the dingo might also be reflective of this domestication process. Current genomic data indicate that feralization in the Australian dingo had started approximately 8000 years ago and that remained genetically isolated until around 200 years ago (Zhang et al., 2020). We postulate that the scaling of the dingo's caudate head either reflects an evolutionary lag in the adjustment of scaling attributes or that dingos have co-opted the capabilities afforded by an expanded caudate head into novel environmental and behavioral circumstances that would require error prediction and evaluation of expectations. While speculative, a relatively expanded caudate head preadapted for action evaluation could be co-opted into social reward interactions by extant dingos. Although dingos are solitary in some areas (Corbett & Newsome, 1975), discrete stable packs of 3–12 individuals have been reported (Corbett, 1995) with groups showing rank order and captive groups even displaying male and female dominance hierarchies (Corbett, 1988).

Scaling analyses of the caudate body identified the European wolf and tiger as having relatively larger and relatively smaller than expected caudate body size, respectively. Given the role of the caudate body in action-controlling functions, our observations may reflect natural differences in inhibitory control between tigers and wolves such that different inhibitory controls could lend itself to different adaptive functions during hunting or social interactions. We postulate that ambush hunting likely relies strongly on inhibitory control, as prepotent impulses necessary to initiate the chase stage of the hunting sequence need to be suppressed until the predator is close enough to the prey to initiate an effective chase. The failure to adequately delay this chase sequence until the desire prey is within reach would result in a loss of opportunity to acquire a meal as well as significant wasted energy, which can be disastrous to the animal. It is also possible that differences in the caudate body size between these species might be related to differences in sociality as observed (Bailey et al., 2013; Kleiman, 1967; Mazák, 1981; Sunquist, 1981).

As the caudate head has a role in cognitive and emotional functions (Graff-Radford et al., 2017; Kemp et al., 2013) and the nucleus accumbens (that we included in our anatomical segmentation) is involved in stimulus-driven motivation (Day & Carelli, 2007), we hypothesized that species average group size would scale with the size of the head of the caudate, but no significant relationship was observed.

We did observe a strong, significantly positive relationship between species home range size and the absolute volume of the caudate body, but subsequent analyses revealed that after correcting for brain size, the caudate body size was not significantly correlated with home range. In summary, scaling of the caudate nucleus and its subcomponents was found to be strongly correlated with brain size, while a consistent pattern of deviation from these scaling attributes was observed in the domestic dog.

4.2 | Shape analysis of the caudate nucleus in carnivores

We observed broad similarities in the curvature of the caudate nucleus within each clade. These similarities in curvature are impressive given the marked difference in brain shape and size between species. For example, the tiger brain is almost nine times larger than that of the domestic cat, but the caudate curvatures were almost identical

10969861, 2024, 5, Downloaded from https://onlinelibrary.wiley.com/doi/10.1002/cne.25618 by South African Medical Research, Wiley Online Library on [31/07/2024]. See the Terms and Conditions (https://onlinelibrary.wiley.com/terms-and-conditions) on Wiley Online Library for rules of use; OA articles are governed by the applicable Creative Commons License

between species. Similarly, we observed a fairly consistent patterning of curvature across the canids; however, a notable difference among canids was the observation of a consistent area of high curvature in the rostral surface of the caudate in the domestic dogs. Given recent functional imaging data on the canine brain (Berns et al., 2012, 2013, 2015) as well as our data reporting relatively expanded caudate dimensions in the domestic dog, it appears that our observations of curvature differences are consistent with the view that the canine caudate has undergone some form of rostral expansion.

We interpret the results of the cross-sectional structural analysis as emphasizing the consistency in structural properties of the caudate across species, with marked weakness in the posterior body and tail of the caudate across canids and felids. Despite this consistency, we also noted that the caudate nucleus of the fennec fox had a large area of maximum weakness/fracture extending into the mid caudate body and head area. This relative extension of the fracture points into the mid caudate body was also observed in the domestic cat albeit to a much lesser extent. Both the fennec fox and the domestic cat had the smallest absolute brain size and caudate size of all the species included in this sample; thus, the expanded fracture points and mesh weakness reported in these two species may be indicative of this diminished absolute brain size. Although the application of this approach in the current study was mainly exploratory, we anticipate several other potential users of this approach for comparative studies. Animal models of traumatic brain injury have shown that models that account for the injury of subcortical structures (e.g., striatum, hippocampus, amygdala, and thalamus) in addition to focal cortical contusions produce symptoms that more closely align with that observed in humans (Thompson et al., 2005; Xiong et al., 2013). Although neuroscientists have predominantly considered mechanical modeling when investigating brain or spinal cord injury (Li et al., 2011), recent studies have shown that mechanical processes play a critical role in neuronal function as well as the control of developmental processes and disease progression (e.g., Barnes et al., 2017; Budday et al., 2014; Goriely et al., 2015; Tyler, 2012). Here we demonstrate that these models can be readily generated to compare features of the 3D neural space in a comparative context.

In conclusion, the evolutionary history of canids and felids is marked by a deep time separation that has uniquely shaped their behavior and phenotype. Our analyses reveal that the scaling and shape characteristics of the caudate nucleus are characterized by conservation within and between these clades, with only slight deviations observed in domestic canids.

AUTHOR CONTRIBUTIONS

Study concept and design: Muhammad A. Spocter, Michael Foster, Paul R. Manger, Chet C. Sherwood. *Collection of and qualitative analysis of data*: Michael Foster, Sai Dwibhashyam, Devan Patel, Kanika Gupta, Brendan K. Billings, Olivia C. Matz, Chet C. Sherwood, and Muhammad A. Spocter. *Statistical analysis and interpretation*: Mary Ann Raghanti, Patrick R. Hof, Chet C. Sherwood, Paul R. Manger, and Muhammad A. Spocter. *Procurement, preparation, and fixation of tissue*: Kathleen Bitterman, Mads Bertelson, Rogier B. Mars, Cheuk Y. Tang, Chet C. Sherwood, Paul R. Manger, and Muhammad A. Spocter. *Obtained funding*: Muhammad A. Spocter and Paul R. Manger. *Drafting of the manuscript*: Muhammad A. Spocter, Paul R. Manger, Chet C. Sherwood, Patrick R. Hof, Rogier B. Mars, and Mary Ann Raghanti. *Photomicrography and preparation of figures/tables*: Michael Foster, Sai Dwibhashyam, Devan Patel, Kanika Gupta, and Muhammad A. Spocter. *Critical revision of the manuscript for important intellectual content*: Muhammad A. Spocter, Paul R. Manger, Chet C. Sherwood, Patrick R. Hof, Rogier B. Mars, and Mary Ann Raghanti. *Study supervision*: Muhammad A. Spocter.

ACKNOWLEDGMENTS

We are also grateful for our community partnership with the Des Moines School District (Central Campus) which has helped to foster interest in STEM fields through supporting high school student involvement in our research. This work was supported by funding from the Iowa STEM BEST (MAS), the South African National Research Foundation (PRM) and the Carnegie-Wits Alumni Diaspora Program through the Carnegie Corporation of New York (MAS and PRM). The work of RBM is supported by the Biotechnology and Biological Sciences Research Council (BBSRC) UK (BB/N019814/1).

CONFLICT OF INTEREST STATEMENT

The authors declare no conflicts of interest.

DATA AVAILABILITY STATEMENT

All quantitative data have been included in the manuscript and imaging data can be provided upon request.

ORCID

Mary Ann Raghanti https://orcid.org/0000-0002-6842-1907
Paul R. Manger https://orcid.org/0000-0002-1881-2854
Muhammad A. Spocter https://orcid.org/0000-0003-1174-7444

PEER REVIEW

The peer review history for this article is available at https://publons.com/publon/10.1002/cne.25618.

REFERENCES

Alexander, G. E., & Crutcher, M. D. (1990). Functional architecture of basal ganglia circuits: Neural substrates of parallel processing. *Trends in Neurosciences*, *13*(7), 266–271.

Andics, A., Gábor, A., Gácsi, M., Faragó, T., Szabó, D., & Miklósi, Á. (2016). Neural mechanisms for lexical processing in dogs. *Science*, *353*(6303), 1030–1032.

Andics, A., & Miklósi, Á. (2018). Neural processes of vocal social perception: Dog-human comparative fMRI studies. *Neuroscience and Biobehavioral Reviews*, *85*, 54–64.

Bailey, I., Myatt, J. P., & Wilson, A. M. (2013). Group hunting within the Carnivora: Physiological, cognitive and environmental influences on strategy and cooperation. *Behavioral Ecology and Sociobiology*, *67*, 1–17.

Balleine, B. W., Delgado, M. R., & Hikosaka, O. (2007). The role of the dorsal striatum in reward and decision-making. *Journal of Neuroscience*, *27*(31), 8161–8165.

Barnes, J. M., Przybyla, L., & Weaver, V. M. (2017). Tissue mechanics regulate brain development, homeostasis and disease. *Journal of Cell Science*, *130*(1), 71–82.

10969861, 2024, 5, Downloaded from https://onlinelibrary.wiley.com/doi/10.1002/cne.25618 by South African Medical Research, Wiley Online Library on [31/07/2024]. See the Terms and Conditions (https://onlinelibrary.wiley.com/terms-and-conditions) on Wiley Online Library for rules of use; OA articles are governed by the applicable Creative Commons License

Batchelor, P. G., Smith, A. C., Hill, D. L., Hawkes, D. J., Cox, T. C., & Dean, A. F. (2002). Measures of folding applied to the development of the human fetal brain. *IEEE Transactions on Medical Imaging*, *21*(8), 953–965.

Berns, G. S., Brooks, A., & Spivak, M. (2013). Replicability and heterogeneity of awake unrestrained canine fMRI responses. *PLoS ONE*, *8*, e81698.

Berns, G. S., Brooks, A. M., & Spivak, M. (2012). Functional MRI in awake unrestrained dogs. *PLoS ONE*, *7*, e38027.

Berns, G. S., Brooks, A. M., & Spivak, M. (2015). Scent of the familiar: An fMRI study of canine brain responses to familiar and unfamiliar human and dog odors. *Behavioural Processes*, *110*, 37–46.

Bininda-Emonds, O. R., Cardillo, M., Jones, K. E., MacPhee, R. D., Beck, R. M., Grenyer, R., Price, S. A., Vos, R. A., Gittleman, J. L., & Purvis, A. (2007). The delayed rise of present-day mammals. *Nature*, *446*(7135), 507–512.

Bininda-Emonds, O. R. P., Cardillo, M., Jones, K. E., MacPhee, R. D. E., Beck, R. M. D., Grenyer, R., Price, S. A., Vos, R. A., Gittleman, J. L., & Purvis, A. (2008). Corrigendum. The delayed rise of present-day mammals. *Nature*, *456*, 274.

Bräuer, J., Kaminski, J., Riedel, J., Call, J., & Tomasello, M. (2006). Making inferences about the location of hidden food: Social dog, causal ape. *Journal of Comparative Psychology*, *120*(1), 38.

Budday, S., Raybaud, C., & Kuhl, E. (2014). A mechanical model predicts morphological abnormalities in the developing human brain. *Scientific Reports*, *4*(1), 5644.

Bush, E. C., & Allman, J. M. (2004). The scaling of frontal cortex in primates and carnivores. *Proceedings of the National Academy of Sciences USA*, *101*(11), 3962–3966.

Chengetanai, S., Tenley, J. D., Bertelsen, M. F., Hård, T., Bhagwandin, A., Haagensen, M., Tang, C. Y., Wang, V. X., Wicinski, B., Hof, P. R., Manger, P. R., & Spocter, M. A. (2020). Brain of the African wild dog. I. Anatomy, architecture, and volumetrics. *Journal of Comparative Neurology*, *528*(18), 3245–3261.

Chiek, V. (2006). Geodesic on surfaces of constant Gaussian curvature [Theses Digitization Project. 3045]. https://scholarworks.lib.csusb.edu/etd-project/3045

Christie, L. A., Saunders, R. C., Kowalska, D. M., MacKay, W. A., Head, E., Cotman, C. W., & Milgram, N. W. (2008). Rhinal and dorsolateral prefrontal cortex lesions produce selective impairments in object and spatial learning and memory in canines. *Journal of Comparative Neurology*, *511*(2), 257–270.

Cook, P. F., & Berns, G. (2022). Volumetric and connectivity assessment of the caudate nucleus in California sea lions and coyotes. *Animal Cognition*, *25*(5), 1231–1240.

Cook, P. F., Prichard, A., Spivak, M., & Berns, G. S. (2016). Awake canine fMRI predicts dogs' preference for praise vs food. *Social Cognitive and Affective Neuroscience*, *11*(12), 1853–1862.

Cook, P. F., Spivak, M., & Berns, G. S. (2014). One pair of hands is not like another: Caudate BOLD response in dogs depends on signal source and canine temperament. *PeerJ*, *2*, e596.

Corbett, L. K. (1988). Social dynamics of a captive dingo pack: Population regulation by dominant female infanticide. *Ethology*, *78*(3), 177–198.

Corbett, L. K. (1995). *The dingo in Australia and Asia*. Sydney, University of New South Wales Press.

Corbett, L. K., & Newsome, A. (1975). Dingo society and its maintenance a preliminary analysis. In M. W. Fox (Ed.), *Wild canid. Their systematics, behavioral ecology and evolution* (pp. 369–379). Van Nostrand Reinhold Company.

Cuaya, L. V., Hernández-Pérez, R., & Concha, L. (2016). Our faces in the Dog's brain: Functional imaging reveals temporal cortex activation during perception of human faces. *PLoS ONE*, *11*(3), e0149431.

Daw, N. D., Gershman, S. J., Seymour, B., Dayan, P., & Dolan, R. J. (2011). Model-based influences on humans' choices and striatal prediction errors. *Neuron*, *69*(6), 1204–1215.

Day, J. J., & Carelli, R. M. (2007). The nucleus accumbens and Pavlovian reward learning. *The Neuroscientist*, *13*(2), 148–159.

Dayer, A. G., Cleaver, K. M., Abouantoun, T., & Cameron, H. A. (2005). New GABAergic interneurons in the adult neocortex and striatum are generated from different precursors. *The Journal of Cell Biology*, *168*(3), 415–427.

Deacon, T. W., Pakzaban, P., & Isacson, O. (1994). The lateral ganglionic eminence is the origin of cells committed to striatal phenotypes: Neural trans- plantation and developmental evidence. *Brain Research*, *668*, 211–219.

Demirci, N., & Holland, M. A. (2022). Cortical thickness systematically varies with curvature and depth in healthy human brains. *Human Brain Mapping*, *43*(6), 2064–2084.

Divac, I. (1972). Delayed alternation in cats with lesions of the prefrontal cortex and the caudate nucleus. *Physiology & Behavior*, *8*, 519–522.

Divac, I. (1974). Caudate nucleus and relearning of delayed alternations in cats. *Physiological Psychology*, *2*, 104–106.

Divac, I., Rosvold, H. E., & Szwarcbart, M. K. (1967). Behavioral effects of selective ablation of the caudate nucleus. *Journal of Comparative and Physiological Psychology*, *63*, 183–190.

Doi, T., Fan, Y., Gold, J. I., & Ding, L. (2020). The caudate nucleus contributes causally to decisions that balance reward and uncertain visual information. *Elife*, *9*, e56694.

Douaud, G., Gaura, V., Ribeiro, M. J., Lethimonnier, F., Maroy, R., Verny, C., Krystkowiak, P., Damier, P., Bachoud-Levi, A. C., Hantraye, P., & Remy, P. (2006). Distribution of grey matter atrophy in Huntington's disease patients: a combined ROI-based and voxel-based morphometric study. *Neuroimage*, *32*(4), 1562–1575.

Emerton, B. C., Jerram, M., Deckersbach, T., Dougherty, D. D., Fulwiler, C., & Gansler, D. A. (2009). A comparison of voxel-based morphometry and volumetry methods in the context of the neural basis of aggression. *Brain Imaging and Behavior*, *3*, 332–341.

Ernst, A., Alkass, K., Bernard, S., Salehpour, M., Perl, S., Tisdale, J., Possnert, G., Druid, H., & Frisén, J. (2014). Neurogenesis in the striatum of the adult human brain. *Cell*, *156*(5), 1072–1083.

Fisher, H. E., Aron, A., & Brown, L. L. (2006). Romantic love: A mammalian brain system for mate choice. *Philosophical Transactions of the Royal Society B: Biological Sciences*, *361*(1476), 2173–2186.

Frysz, W., & Stepien, I. (1983). Function of cat's caudate nucleus in tasks involving spatial discontinuity between location of cue and response. *Acta Neurobiologiae Experimentalis*, *43*, 103–113.

Goldman, P. S., & Rosvold, H. E. (1970). Localization of function within the dorsolateral prefrontal cortex in the rhesus monkey. *Experimental Neurology*, *27*, 2304–2911.

Goriely, A., Geers, M. G., Holzapfel, G. A., Jayamohan, J., Jérusalem, A., Sivaloganathan, S., Squier, W., van Dommelen, J. A., Waters, S., & Kuhl, E. (2015). Mechanics of the brain: Perspectives, challenges, and opportunities. *Biomechanics and Modeling in Mechanobiology*, *14*, 931–965.

Graff-Radford, J., Williams, L., Jones, D. T., & Benarroch, E. E. (2017). Caudate nucleus as a component of networks controlling behavior. *Neurology*, *89*, 2192.

Grahn, J. A., Parkinson, J. A., & Owen, A. M. (2008). The cognitive functions of the caudate nucleus. *Progress in Neurobiology*, *86*(3), 141–155.

Grewal, J. S., Gloe, T., Hegedus, J., Bitterman, K., Billings, B. K., Chengetanai, S., Bentil, S., Wang, V. X., Ng, J. C., Tang, C. Y., Geletta, S., Wicinski, B., Bertelson, M., Tendler, B. C., Mars, R. B., Aguirre, G. K., Rusbridge, C., Hof, P. R., Sherwood, C. C., … Spocter, M. A. (2020). Brain gyrification in wild and domestic canids: Has domestication changed the gyrification index in domestic dogs? *Journal of Comparative Neurology*, *528*(18), 3209–3228.

Haber, S. N. (2003). The primate basal ganglia: Parallel and integrative networks. *Journal of Chemical Neuroanatomy*, *26*, 317–330.

Haber, S. N., Kunishio, K., Mizobuchi, M., & Lynd-Balta, E. (1995). The orbital and medial prefrontal circuit through the primate basal ganglia. *Journal of Neuroscience*, *15*, 4851–4867.

Hare, B., Call, J., & Tomasello, M. (1998). Communication of food location between human and dog (*Canis familiaris*). *Evolution of Communication*, *2*(1), 137–159.

10969861, 2024, 5, Downloaded from https://onlinelibrary.wiley.com/doi/10.1002/cne.25618 by South African Medical Research, Wiley Online Library on [31/07/2024]. See the Terms and Conditions (https://onlinelibrary.wiley.com/terms-and-conditions) on Wiley Online Library for rules of use; OA articles are governed by the applicable Creative Commons License

Hare, B., & Tomasello, M. (2005). Human-like social skills in dogs? *Trends in Cognitive Sciences*, *9*(9), 439–444.

Hecht, E. E., Kukekova, A. V., Gutman, D. A., Acland, G. M., Preuss, T. M., & Trut, L. N. (2021). Neuromorphological changes following selection for tameness and aggression in the Russian fox-farm experiment. *Journal of Neuroscience*, *41*(28), 6144–6156.

Hecht, E. E., Smaers, J. B., Dunn, W. D., Kent, M., Preuss, T. M., & Gutman, D. A. (2019). Significant neuroanatomical variation among domestic dog breeds. *Journal of Neuroscience*, *39*(39), 7748–7758.

Hikosaka, O., Takikawa, Y., & Kawagoe, R. (2000). Role of the basal ganglia in the control of purposive saccadic eye movements. *Physiological Reviews*, *80*(3), 953–978.

Huber, L., & Lamm, C. (2017). Understanding dog cognition by functional magnetic resonance imaging. *Learning & Behavior*, *45*, 101–102.

Hynd, G. W., Hern, K. L., Ovey, E. S., Eliopulos, D., Marshall, R., Gonzalez, J. J., & Voeller, K. K. (1993). Attention deficit hyperactivity disorder and asymmetric of the caudate nucleus. *Journal of Child Neurology*, *8*, 339–347.

Isaacs, E. B., Gadian, D. G., Sabatini, S., Chong, W. K., Quinn, B. T., Fischl, B. R., & Lucas, A. (2008). The effect of early human diet on caudate volumes and IQ. *Pediatric research*, *63*(3), 308–314.

Izuma, K., Saito, D. N., & Sadato, N. (2008). Processing of social and monetary rewards in the human striatum. *Neuron*, *58*(2), 284–294.

Jacobs, B., Garcia, M. E., Shea-Shumsky, N. B., Tennison, M. E., Schall, M., Saviano, M. S., Tummino, T. A., Bull, A. J., Driscoll, L. L., Raghanti, M. A., Lewandowski, A. H., Wicinski, B., Ki Chui, H., Bertelsen, M. F., Walsh, T., Bhagwandin, A., Spocter, M. A., Hof, P. R., Sherwood, C. C., & Manger, P. R. (2018). Comparative morphology of gigantopyramidal neurons in primary motor cortex across mammals. *Journal of Comparative Neurology*, *526*(3), 496–536.

Jardim-Messeder, D., Lambert, K., Noctor, S., Pestana, F. M., de Castro Leal, M. E., Bertelsen, M. F., Walsh, T., Bhagwandin, A., Spocter, M. A., Hof, P. R., Sherwood, C. C., & Herculano-Houzel, S. (2017). Dogs have the most neurons, though not the largest brain: Trade-off between body mass and number of neurons in the cerebral cortex of large carnivoran species. *Frontiers in Neuroanatomy*, *11*, 118.

Jia, H., Pustovyy, O. M., Waggoner, P., Beyers, R. J., Schumacher, J., Wildey, C., Barrett, J., Morrison, E., Salibi, N., Denney, T. S., Vodyanoy, V. J., & Deshpande, G. (2014). Functional MRI of the olfactory system in conscious dogs. *PLoS ONE*, *9*(1), e86362.

Juh, R., Su, M., Lee, C., Suh, T., & Nalcioglu, O. (2006). Investigate between the voxel based morphometry and regions of interest study in Alzheimer's disease. *Medical Physics*, *33*, 2020.

Karl, S., Boch, M., Zamansky, A., van der Linden, D., Wagner, I. C., Völter, C. J., Lamm, C., & Huber, L. (2020). Exploring the dog-human relationship by combining fMRI, eye-tracking and behavioural measures. *Scientific Reports*, *10*(1), 22273.

Kemp, J., Berthel, M. C., Dufour, A., Després, O., Henry, A., Namer, I. J., Musacchio, M., & Sellal, F. (2013). Caudate nucleus and social cognition: Neuropsychological and SPECT evidence from a patient with focal caudate lesion. *Cortex; A Journal Devoted to the Study of the Nervous System and Behavior*, *49*, 559–571.

Kleiman, D. G. (1967). Some aspects of social behavior in the *Canidae*. *American Zoologist*, *7*(2), 365–372.

Knutson, B., Adams, C. M., Fong, G. W., & Hommer, D. (2001). Anticipation of increasing monetary reward selectively recruits nucleus accumbens. *The Journal of Neuroscience*, *21*(16), RC159.

Koob, G. F. (1992). Drugs of abuse: Anatomy, pharmacology and function of reward pathways. *Trends in Pharmacological Sciences*, *13*, 177–184.

Kotz, S. A., Anwander, A., Axer, H., & Knösche, T. R. (2013). Beyond cytoarchitectonics: The internal and external connectivity structure of the caudate nucleus. *PLoS ONE*, *8*(7), e70141.

Kruska, V. D. (1980). Domestikationsbedingte Hirngrößenanderungen bei Säugetieren. *Journal of Zoological Systematics and Evolutionary Research*, *18*(3), 161–195.

Lauwereyns, J., Watanabe, K., Coe, B., & Hikosaka, O. (2002). A neural correlate of response bias in monkey caudate nucleus. *Nature*, *418*(6896), 413–417.

Lawicka, W. (1972). Proreal syndrome in dogs. *Acta Neurobiologiae Experimentalis*, *32*, 261–276.

Lawicka, W., Mishkin, M., & Rosvold, H. E. (1975). Dissociation of deficits on auditory tasks following partial prefrontal lesions in monkeys. *Acta Neurobiologiae Experimentalis*, *35*, 581–4307.

Lawrence, A. D., Sahakian, B. J., & Robbins, T. W. (1998). Cognitive functions and corticostriatal circuits: Insights from Huntington's disease. *Trends in Cognitive Sciences*, *2*(10), 379–388.

Levitt, J. J., McCarley, R. W., Dickey, C. C., Voglmaier, M. M., Niznikiewicz, M. A., Seidman, L. J., Hirayasu, Y., Ciszewski, A. A., Kikinis, R., Jolesz, F. A., & Shenton, M. E. (2002). MRI study of caudate nucleus volume and its cognitive correlates in neuroleptic-naive patients with schizotypal personality disorder. *Am J Psychiatry*, *159*(7), 1190–1197.

Li, X., von Holst, H., & Kleiven, S. (2011). Influence of gravity for optimal head positions in the treatment of head injury patients. *Acta Neurochirurgica*, *153*, 2057–2064.

Lin, L. I. (1989). A concordance correlation coefficient to evaluate reproducibility. *Biometrics*, *45*, 225–268.

Lou, H. C., Henriksen, L., Bruhn, P., Børner, H., & Nielsen, J. B. (1989). Striatal dysfunction in attention deficit and hyperkinetic disorder. *Archives of Neurology*, *46*(1), 48–52.

Luzzati, F., De Marchis, S., Fasolo, A., & Peretto, P. (2006). Neurogenesis in the caudate nucleus of the adult rabbit. *Journal of Neuroscience*, *26*(2), 609–621.

Lyras, G. A. (2009). The evolution of the brain in *Canidae* (Mammalia: Carnivora). *Scripta Geologica*, *139*, 1–93.

Mai, J. K., Voss, T., & Paxinos, G. (2015). *Atlas of the human brain* (4th ed.). Academic Press.

Manger, P. R., Spocter, M. A., & Patzke, N. (2013). The evolutions of large brain size in mammals: The 'over-700-gram club quartet'. *Brain Behavior and Evolution*, *82*(1), 68–78.

Matz, O. C., & Spocter, M. (2022). The effect of Huntington's disease on the basal Nuclei: A review. *Cureus*, *14*(4), e24473.

Mazák, V. (1981). Panthera tigris. *Mammalian Species*, *152*, 1–8.

McKinley, J., & Sambrook, T. D. (2000). Use of human-given cues by domestic dogs (*Canis familiaris*) and horses (*Equus caballus*). *Animal Cognition*, *3*, 13–22.

Michaud, M., Toussaint, S. L. D., & Gilissen, E. (2022). The impact of environmental factors on the evolution of brain size in carnivorans. *Communications Biology*, *5*, 998.

Middleton, F. A., & Strick, P. L. (1996). The temporal lobe is a target of output from the basal ganglia. *Proceedings of the National Academy of Sciences USA*, *93*(16), 8683–8687.

Miklösi, Á., Polgárdi, R., Topál, J., & Csányi, V. (1998). Use of experimenter-given cues in dogs. *Animal Cognition*, *1*, 113–121.

Mishkin, M., & Pribram, K. H. (1954). Visual discrimination performance following partial ablations of the temporal lobe. I. Ventral vs lateral. *Journal of Comparative and Physiological Psychology*, *47*, 14–20.

Montague, P. R., & Berns, G. S. (2002). Neural economics and the biological substrates of valuation. *Neuron*, *36*(2), 265–284.

Nambu, A. (2008). Seven problems on the basal ganglia. *Current Opinion in Neurobiology*, *18*(6), 595–604.

Nelson, J., Woeste, E. M., Oba, K., Bitterman, K., Billings, B. K., Sacco, J., Jacobs, B., Sherwood, C. C., Manger, P. R., & Spocter, M. A. (2024). Neuropil variation in the prefrontal, motor, and visual cortex of six felids. *Brain Behavior and Evolution*, *00*, 00. https://doi.org/10.1159/000537843

Nguyen, V. T., Uchida, R., Warling, A., Sloan, L. J., Saviano, M. S., Wicinski, B., Hård, T., Bertelsen, M. F., Stimpson, C. D., Bitterman, K., Schall, M., Hof, P. R., Sherwood, C. C., Manger, P. R., Spocter, M. A., & Jacobs, B. (2020). Comparative neocortical neuromorphology in felids: African lion, African leopard, and cheetah. *Journal of Comparative Neurology*, *528*(8), 1392–1422.

10969861, 2024, 5, Downloaded from https://onlinelibrary.wiley.com/doi/10.1002/cne.25618 by South African Medical Research, Wiley Online Library on [31/07/2024]. See the Terms and Conditions (https://onlinelibrary.wiley.com/terms-and-conditions) on Wiley Online Library for rules of use; OA articles are governed by the applicable Creative Commons License

Nowak, R. M. (2005). *Walker's carnivores of the world*. Johns Hopkins University Press.

Nyakatura, K., & Bininda-Emonds, O. R. (2012). Updating the evolutionary history of Carnivora (Mammalia): A new species-level supertree complete with divergence time estimates. *BMC Biology*, *10*, 1–31.

Oddes, D., Ngwenya, A., Malungo, I. B., Burkevica, A., Hård, T., Bertelsen, M. F., Spocter, M. A., Scantlebury, D. M., & Manger, P. R. (2023). Orexinergic neurons in the hypothalami of an Asiatic lion, an African lion, and a Southeast African cheetah. *Journal of Comparative Neurology*, *531*(3), 366–389.

Olmstead, C. E., & Villablanca, J. R. (1979). Effects of caudate nuclei or frontal cortical ablations in kittens: Bar pressing performance. *Experimental Neurology*, *63*, 244–256.

Olmstead, C. E., Villablanca, J. R., Marcus, R. J., & Avery, D. L. (1976). Effects of caudate nuclei or frontal cortex ablations in cats. IV. Bar pressing, maze learning, and performance. *Experimental Neurology*, *53*, 670–693.

Onorati, M., Castiglioni, V., Biasci, D., Cesana, E., Menon, R., Vuono, R., Talpo, F., Laguna Goya, R., Lyons, P. A., Bulfamante, G. P., Muzio, L., Martino, G., Toselli, M., Farina, C., Barker, R. A., Biella, G., & Cattaneo, E. (2014). Molecular and functional definition of the developing human striatum. *Nature Neuroscience*, *12*, 1804–1815.

Orme, C. D. L., Freckleton, R. P., Thomas, G. H., Petzoldt, T., Fritz, S. A., & Isaac, N. J. B. (2013). Caper: Comparative analyses of phylogenetics and evolution in R. *Methods in Ecology and Evolution*, *3*, 145–151.

Palazzi, X. (2011). *The Beagle brain in stereotaxic coordinates*. (11th ed.). Springer.

Pienaar, R., Fischl, B., Caviness, V., Makris, N., & Grant, P. E. (2008). A methodology for analyzing curvature in the developing brain from preterm to adult. *International Journal of Imaging Systems and Technology*, *18*(1), 42–68.

Podbros, L. Z., Stamm, J. S., & Denaro, F. J. (1980). Associative function of the arcuate segment of the monkey's prefrontal cortex. *Physiology & Behavior*, *24*, 103–109.

Potegal, M. (1972). The caudate nucleus egocentric localization system. *Acta Neurobiologiae Experimentalis*, *32*, 479–494.

Pribram, K. H., Mishkin, M., Rosvold, H. E., & Kaplan, S. J. (1952). Effects on delayed response performance of lesions of dorsolateral and ventromedial cortex of baboons. *Journal of Comparative and Physiological Psychology*, *45*, 565–575.

Rilling, J. K., Gutman, D. A., Zeh, T. R., Pagnoni, G., Berns, G. S., & Kilts, C. D. (2002). A neural basis for social cooperation. *Neuron*, *35*(2), 395–405.

Robinson, D., Wu, H., Munne, R. A., Ashtari, M., Alvir, J. M. J., Lerner, G., Koreen, A., Cole, K., & Bogerts, B. (1995). Reduced caudate nucleus volume in obsessive-compulsive disorder. *Archives of General Psychiatry*, *52*(5), 393–398.

Röhrs, M., & Ebinger, P. (1978). Die Beurteilung von Hirngrößenunterschieden zwischen Wild-und Haustieren. *Journal of Zoological Systematics and Evolutionary Research*, *16*(1), 1–14.

Ronan, L., Pienaar, R., Williams, G., Bullmore, E. D., Crow, T. J., Roberts, N., Jones, P. B., Suckling, J., & Fletcher, P. C. (2011). Intrinsic curvature: A marker of millimeter-scale tangential cortico-cortical connectivity? *International Journal of Neural Systems*, *21*(05), 351–366.

Ronan, L., Voets, N., Rua, C., Alexander-Bloch, A., Hough, M., Mackay, C., Crow, T. J., James, A., Giedd, J. N., & Fletcher, P. C. (2014). Differential tangential expansion as a mechanism for cortical gyrification. *Cerebral Cortex*, *24*(8), 2219–2228.

Sacco, J. C., Starr, E., Weaver, A., Dietz, R., & Spocter, M. A. (2023). Resequencing of the TMF-1 (TATA Element Modulatory Factor) regulated protein (TRNP1) gene in domestic and wild canids. *Canine Med Genet*, *10*(1), 10.

Scarone, S., Colombo, C., Livian, S., Abbruzzese, M., Ronchi, P., Locatelli, M., Scotti, G., & Smeraldi, E. (1992). Increased right caudate nucleus size in obsessive-compulsive disorder: Detection with magnetic resonance imaging. *Psychiatry Research: Neuroimaging*, *45*(2), 115–121.

Schleifenbaum, C. (1973). The postnatal development of the brain of poodles and wolves (author's transl). *Zeitschrift Fur Anatomie Und Entwicklungsgeschichte*, *141*, 179–205.

Schultz, W., Dayan, P., & Montague, P. R. (1997). A neural substrate of prediction and reward. *Science*, *275*(5306), 1593–1599.

Sears, L. L., Vest, C., Mohamed, S., Bailey, J., Ranson, B. J., & Piven, J. (1999). An MRI study of the basal ganglia in autism. *Progress in Neuro-psychopharmacology & Biological Psychiatry*, *23*(4), 613–624.

Seger, C. A., & Cincotta, C. M. (2005). The roles of the caudate nucleus in human classification learning. *Journal of Neuroscience*, *25*(11), 2941–2951.

Sheppard, D. M., Bradshaw, J. L., Purcell, R., & Pantelis, C. (1999). Tourette's and comorbid syndromes: Obsessive compulsive and attention deficit hyperactivity disorder. A common etiology? *Clinical Psychology Review*, *19*(5), 531–552.

Shimony, J. S., Smyser, C. D., Wideman, G., Alexopoulos, D., Hill, J., Harwell, J., Dierker, D., van Essen, D. C., Inder, T. E., & Neil, J. J. (2016). Comparison of cortical folding measures for evaluation of developing human brain. *Neuroimage*, *125*, 780–790.

Spocter, M. A., Uddin, A., Ng, J. C., Wong, E., Wang, V. X., Tang, C., Wicinski, B., Haas, J., Bitterman, K., Raghanti, M. A., Dunn, R., Hof, P. R., Sherwood, C. C., Jovanovik, J., Rusbridge, C., & Manger, P. R. (2018). Scaling of the corpus callosum in wild and domestic canids: Insights into the domesticated brain. *Journal of Comparative Neurology*, *526*(15), 2341–2359.

Stepien, I., Stepien, L., & Sychowa, B. (1966). Disturbances of motor conditioned behavior following bilateral ablations of the precruciate area in dogs and cats. *Acta Neurobiologiae Experimentalis*, *26*, 323–340.

Stephan, H. (1960). Methodische Studien über den quantitativen Vergleich architektonischer Struktureinheiten des Gehirns. *Z Wiss Zool.*, *164*, 143–172.

Stepien, I., Stepien, L., & Toeplitz, Z. (1975). Prefrontal cortex and manipulatory go-left, go-right differentiation to acoustic directional cues in dogs. *Acta Neurobiologiae Experimentalis*, *35*, 537–548.

Sunquist, M. E. (1981). *The social organization of tigers (Panthera* tigris*) in Royal Chitawan National park, Nepal*. https://doi.org/10.5479/si.00810282.336

Tanaka, S. C., Balleine, B. W., & O'Doherty, J. P. (2008). Calculating consequences: Brain systems that encode the causal effects of actions. *Journal of Neuroscience*, *28*(26), 6750–6755.

Tanaka, S. C., Samejima, K., Okada, G., Ueda, K., Okamoto, Y., Yamawaki, S., & Doya, K. (2006). Brain mechanism of reward prediction under predictable and unpredictable environmental dynamics. *Neural Networks*, *19*(8), 1233–1241.

Tensen, L. (2018). Biases in wildlife and conservation research, using felids and canids as a case study. *Global Ecology and Conservation*, *15*, e00423.

Thompson, H. J., Lifshitz, J., Marklund, N., Grady, M. S., Graham, D. I., Hovda, D. A., & McIntosh, T. K. (2005). Lateral fluid percussion brain injury: A 15-year review and evaluation. *Journal of Neurotrauma*, *22*(1), 42–75.

Tyler, W. J. (2012). The mechanobiology of brain function. *Nature Reviews Neuroscience*, *13*(12), 867–878.

van Valkenberg, B. (1985). Locomotor diversity within past and present guilds of large predatory mammals. *Paleobiology*, *11*(4), 406–428.

Villablanca, J. R. (2010). Why do we have a caudate nucleus. *Acta Neurobiologiae Experimentalis (Wars)*, *70*(1), 95–105.

Villablanca, J. R., Olmstead, C. E., Levine, M. S., & Marcus, R. J. (1978). Effects of caudate nuclei or frontal cortical ablations in kittens: Neurology and gross behavior. *Experimental Neurology*, *61*, 615–634.

White, N. M. (2009). Some highlights of research on the effects of caudate nucleus lesions over the past 200 years. *Behavioral Brain Research*, *199*, 3–23.

Wise, S. P., Murray, E. A., & Gerfen, C. R. (1996). The frontal cortex-basal ganglia system in primates. *Critical Reviews in Neurobiology*, *10*(3–4), 317–356.

Xiong, Y., Mahmood, A., & Chopp, M. (2013). Animal models of traumatic brain injury. *Nature Reviews Neuroscience*, *14*(2), 128–142.

10969861, 2024, 5, Downloaded from https://onlinelibrary.wiley.com/doi/10.1002/cne.25618 by South African Medical Research, Wiley Online Library on [31/07/2024]. See the Terms and Conditions (https://onlinelibrary.wiley.com/terms-and-conditions) on Wiley Online Library for rules of use; OA articles are governed by the applicable Creative Commons License

Yanike, M., & Ferrera, V. P. (2014). Representation of outcome risk and action in the anterior caudate nucleus. *Journal of Neuroscience*, *34*(9), 3279–3290.

Yushkevich, P. A., Piven, J., Hazlett, H. C., Smith, R. G., Ho, S., Gee, J. C., & Gerig, G. (2006). User-guided 3D active contour segmentation of anatomical structures: Significantly improved efficiency and reliability. *Neuroimage*, *31*(3), 1116–1128.

Zhang, S. J., Wang, G. D., Ma, P., Zhang, L. L., Yin, T. T., Liu, Y. H., Otecko, N. O., Wang, M., Ma, Y. P., Wang, L., Mao, B., Savolainen, P., & Zhang, Y. P. (2020). Genomic regions under selection in the feralization of the dingoes. *Nature Communications*, *11*(1), 671.

How to cite this article: Foster, M., Dwibhashyam, S., Patel, D., Gupta, K., Matz, O. C., Billings, B. K., Bitterman, K., Bertelson, M., Tang, C. Y., Mars, R. B., Raghanti, M. A., Hof, P. R., Sherwood, C. C., Manger, P. R., & Spocter, M. A. (2024). Comparative anatomy of the caudate nucleus in canids and felids: Associations with brain size, curvature, cross-sectional properties, and behavioral ecology. *Journal of Comparative Neurology*, *532*, e25618. https://doi.org/10.1002/cne.25618

10969861, 2024, 5, Downloaded from https://onlinelibrary.wiley.com/doi/10.1002/cne.25618 by South African Medical Research, Wiley Online Library on [31/07/2024]. See the Terms and Conditions (https://onlinelibrary.wiley.com/terms-and-conditions) on Wiley Online Library for rules of use; OA articles are governed by the applicable Creative Commons License